Annual Review of Financial Economics

Comparative Valuation Dynamics in Production Economies: Long-Run Uncertainty, Heterogeneity, and Market Frictions

Lars Peter Hansen,[1] Paymon Khorrami,[2] and Fabrice Tourre[3]

[1]Department of Economics, University of Chicago, Chicago, Illinois, USA; email: lhansen@uchicago.edu

[2]The Fuqua School of Business, Duke University, Durham, North Carolina, USA

[3]Department of Economics and Finance, Baruch College, City University of New York, New York, NY, USA

Annu. Rev. Financ. Econ. 2024. 16:1–38

First published as a Review in Advance on September 26, 2024

The *Annual Review of Financial Economics* is online at financial.annualreviews.org

https://doi.org/10.1146/annurev-financial-082123-105652

JEL codes: C68, D45, D53, D81, G12

Keywords

asset pricing, long-run uncertainty, robustness, diversification, heterogeneous agents, market frictions

Abstract

We compare and contrast production economies exposed to long-run uncertainty with investors that have possibly different preferences and/or access to financial markets. We study the macroeconomic and asset-pricing properties of these models, identify common features, and highlight areas where these models depart from each other. Our framework allows us to investigate more fully the impact of investor heterogeneity, capital heterogeneity, and fluctuations of the growth components to the capital evolution as they affect the dynamics of macroeconomic quantities and asset prices. In our comparisons, we employ an array of diagnostic tools to explore time variation and state dependencies in nonlinear environments.

Beware the person of one ~~book~~ model.

—Thomas Aquinas (with the author's edits)

1. INTRODUCTION

An underappreciated task in the study of dynamic macroeconomics is model comparison. This is especially true for models requiring numerical methods to solve and analyze. While journals seemingly embrace publications that target specific models, there is much to be gained by looking formally across models.

One strategy for making comparisons across models is to nest models within a common framework in which each model of interest is a special case. At this juncture, we could turn things over to a statistician to test which model within this nesting best fits the data. This strategy makes the most sense when we could plausibly view one of the models within the family as being correctly specified, given the data. But in many cases, we see models as providing valuable insights even when they are not designed to fit some agreed-upon list of favorite facts. As we explore nonlinear models more fully, this nesting-testing approach becomes all the more challenging. But even for examples when linearized approximations work well, the fitting of all or some predesignated facts can lead to black box outcomes when driven by the simplistic ambitions of full empirical success. Models often end up with multiple pieces clouding the ability to isolate and understand better particular economic mechanisms.

In this article, we develop a framework and diagnostic tools for comparing and contrasting dynamic macroeconomic models. The models that interest us require special attention relative to most dynamic stochastic general equilibrium (DSGE) models because of the important role played by nonlinearity in the implied dynamic evolution. This nonlinearity has notable implications for both economic and financial market outcomes. Given these ambitions, our analysis is explicitly numerical and not limited to paper-and-pencil style analyses. It is necessary that we solve such models using global solution methods, as the competitive equilibrium is typically characterized by a set of highly nonlinear second-order elliptic partial differential equations (PDEs). Moreover, even with the option of numerical solutions, we find it revealing to explore and compare highly stylized models featuring particular economic mechanisms. In accompanying notebooks and user-friendly software, we propose and explore quantitative methods that expose salient features of the macroeconomic and valuation dynamics of the models we investigate. This article provides illustrations of possible computations.

While we explore two different classes of models, a common feature in all of them is a long-run process altering investment opportunities. Our technologies can be viewed as production-based specifications inclusive of long-run risk. Analogous to the work by Bansal & Yaron (2004), we capture this risk with a continuous-time version of a first-order autoregressive process. The process is meant to be a simple proxy for uncertainty of such phenomena as secular stagnation and technological progress or other forms of long-term uncertainty.

The first class of models has no market frictions. While including stochastic growth following in the footsteps of Lucas & Prescott (1971) and Brock & Mirman (1972), these models include a single investor type. We start by considering a model with a single capital stock with a long-run risk contribution to investment opportunities. While we provide some sensitivity analyses that are of interest in their own right, understanding these initial models sets the stage for our subsequent investigations.

We give two extensions, one in which the representative or stand-in investor has concerns about model ambiguity captured by uncertainty in growth-rate persistence along with overall model misspecification concerns. The other extension considers specifications with two capital stocks

differentially exposed to macroeconomic shocks. Capital movements are sluggish in the sense that there are adjustment costs in both capital technologies. This class of models extends those of Eberly & Wang (2009, 2011). We investigate the consequences of heterogeneous technological exposure to long-run risk in conjunction with motives for diversification. Including production in which the two capital stocks are not perfect substitutes adds an additional economic channel with interesting nonlinear impacts.

The second class of models, motivated in part by financial crises like the global financial crisis of 2008, considers two heterogeneous investor types. These agents can differ in skill, preferences, or contractual and regulatory constraints. Dynamic trading between these heterogeneous investors induces potentially dramatic economic and financial market outcomes in some states of the world, especially those in which constraints are binding. Our exercise is motivated by a substantial literature with a variety of different modeling ingredients. These include, for instance, the models from Basak & Cuoco (1998), He & Krishnamurthy (2011), Brunnermeier & Sannikov (2014), and Gârleanu & Panageas (2015). Recently, several papers have exposed a more complex representation of the role of financial intermediation than that captured by the stylized models we consider here. It is not our aim in this article to survey this literature. The models we consider, however, do have mechanisms that enhance our understanding of nonlinear linkages between financial markets and the macroeconomy, even if they miss some of the actual complexities that limit financial intermediaries or other such specialists.

2. INVESTOR PREFERENCES

In this article, we use a continuous-time specification of a Kreps & Porteus (1978) utility recursion as in Duffie & Epstein (1992) in connection with an information structure generated and expressed in terms of a vector standard Brownian motion $B \stackrel{\text{def}}{=} \{B_t : t \geq 0\}$ of dimension d. Thus, we are imposing local normality. While shocks are normally distributed, we entertain nonlinear transition mechanisms that permit endogenously determined variables to possess transition probabilities and stationary distributions that are not even approximately normal. In this section, we provide a heuristic link between the continuous-time and discrete-time representation of preferences, since the discrete-time formulation has been used extensively in the quantitative asset-pricing literature. The local normality does allow for some simplicity when we study continuous time–limiting economies. We do not ask the reader to be knowledgeable of the subtleties associated with the continuous-time mathematics.

2.1. Discrete Time

Continuation values provide a convenient way to specify recursive preferences. With this in mind, let $V \stackrel{\text{def}}{=} \{V_t : t \geq 0\}$ be the continuation utility process, where V_t is a date-t utility index that summarizes current and future prospective contributions to preferences. In discrete time with a time interval ϵ, we use two CES (constant elasticity of substitution) homogeneous of degree-one recursions to represent the evolution of continuation values:

$$V_t = \left[\left[1 - \exp(-\delta\epsilon)\right](C_t)^{1-\rho} + \exp(-\delta\epsilon)\mathbb{R}(V_{t+\epsilon} \mid \mathfrak{F}_t)^{1-\rho}\right]^{\frac{1}{1-\rho}}$$

$$\mathbb{R}(V_{t+\epsilon} \mid \mathfrak{F}_t) = \left(\mathbb{E}\left[(V_{t+\epsilon})^{1-\gamma} \mid \mathfrak{F}_t\right]\right)^{\frac{1}{1-\gamma}}, \qquad 1.$$

where $\mathfrak{F}_t$ is the time-t information set. Notice that the second equation computes a certainty equivalent with parameter γ. If the continuation utility $V_{t+\epsilon}$ is known at t, then γ has no impact on the recursion since $\mathbb{R}(V_{t+\epsilon} \mid \mathfrak{F}_t) = V_{t+\epsilon}$, implying that this contribution is indeed an adjustment

for risk. Taking the two equations together, this is a forward-looking recursion whereby we start with a terminal specification of the continuation utility and work backward. We consider infinite horizon counterparts in our computations. Notice that this recursive specification is governed by three underlying parameters:

1. δ, the subjective discount rate;
2. ρ, the inverse of the intertemporal elasticity of substitution (IES); and
3. γ, the risk aversion.

In some later examples, we will have two investor types with possibly heterogeneous specifications of the preference parameters (δ, ρ, γ). Two special cases of these preferences are: $\rho = \gamma$ and $\rho = 1$. When $\rho = \gamma$, this utility recursion defines preferences that are equivalent to those implied by discounted, time-separable power utility. Specifically, when $\gamma = \rho$, by solving the recursion forward, it follows that

$$V_t = \left(\mathbb{E}\left[\frac{1}{1-\exp(-\delta\epsilon)} \sum_{j=0}^{\infty} \exp(-\delta j\epsilon) \left(C_{t+j\epsilon}\right)^{1-\gamma} \mid \mathfrak{F}_t \right] \right)^{\frac{1}{1-\gamma}}, \quad \text{if} \quad \rho = \gamma. \tag{2.}$$

Imposing $\rho = 1$ implies a unitary IES, and the limiting recursion has a Cobb-Douglas representation:

$$V_t = (C_t)^{[1-\exp(-\delta\epsilon)]} \left[\mathbb{R}(V_{t+\epsilon} \mid \mathfrak{F}_t)\right]^{\exp(-\delta\epsilon)}, \quad \text{if} \quad \rho = 1.$$

Continuation values are only defined up to increasing transformations. Numerical and conceptual convenience lead us to use $\widehat{V}_t = \log V_t$. (We will always use the notation $\widehat{X}$ to designate the logarithm of a variable X.) The logarithmic counterparts to the underlying recursions are given by

$$\widehat{V}_t = \frac{1}{1-\rho} \log\left[\left[1-\exp(-\delta\epsilon)\right](C_t)^{1-\rho} + \exp(-\delta\epsilon)\exp\left[(1-\rho)\widehat{\mathbb{R}}(\widehat{V}_{t+\epsilon} \mid \mathfrak{F}_t)\right]\right]$$

$$\widehat{\mathbb{R}}\left(\widehat{V}_{t+\epsilon} \mid \mathfrak{F}_t\right) = \frac{1}{1-\gamma} \log\left(\mathbb{E}\left[\exp[(1-\gamma)\widehat{V}_{t+\epsilon}] \mid \mathfrak{F}_t\right]\right). \tag{3.}$$

For this representation, $\rho = \gamma = 1$ is a relevant benchmark whereby the recursions become

$$\widehat{V}_t = \left[1-\exp(-\delta\epsilon)\right]\log C_t + \exp(-\delta\epsilon)\widehat{\mathbb{R}}(\widehat{V}_{t+\epsilon} \mid \mathfrak{F}_t)$$

$$\widehat{\mathbb{R}}(\widehat{V}_{t+\epsilon} \mid \mathfrak{F}_t) = \mathbb{E}[\widehat{V}_{t+\epsilon} \mid \mathfrak{F}_t], \tag{4.}$$

which have discounted logarithmic utility scaled by $[1-\exp(-\delta\epsilon)]$ as the solution.

2.2. Robustness to Model Misspecification

Our motivation so far for the recursive utility formulation relies on uncertainty aversion as applying to risk, a situation in which investors have complete confidence in their probability assignments. In many applications, this narrow notion of uncertainty seems like a strain. This especially could be a concern when considering uncertainty in long-term macroeconomic growth rates.[1] Concerns about ambiguity as to which among a family of potential models is one that governs data generation or concerns about potential model misspecification may come into play as reflecting broader notions of uncertainty concerns.[2] We now show how to reinterpret the

[1] See, for instance, discussions by Hansen (2007) and Chen, Dou & Kogan (2024).

[2] For some recent discussions of axiomatic rationales, see Hansen & Sargent (2023) and Cerreia-Vioglio et al. (2024).

recursive utility formulation (Equation 1) as a preference for robustness to model uncertainty. Later in this article, we also consider implications of aversion to ambiguity over how to weigh alternative models (see Section 4.5).

Using the lens of robust control theory, consider a positive random variable $L_{t+\epsilon}$ with unit-conditional expectation—a convenient mathematical device pertinent to models of subjective beliefs that are distinct from those implied by the data-generating process:

$$\mathbb{E}\left(L_{t+\epsilon} \mid \mathfrak{F}_t\right) = 1.$$

Think of $L_{t+\epsilon}$ as a relative density (likelihood ratio) that alters the transition probability from t to $t+\epsilon$. To obtain the implied subjective conditional expectations, multiply the next-period random variables by $L_{t+\epsilon}$ prior to forming the conditional expectations. For instance, the implied subjective expectation of next period's continuation value is $\mathbb{E}(L_{t+\epsilon}\widehat{V}_{t+\epsilon} \mid \mathfrak{F}_t)$.

While a subjective belief specification allows for departures from a rational expectations assumption that investors know the data-generating process, we use the modeling approach differently. Suppose that the investor has a benchmark model of the transition probabilities without full confidence in that specification. This skepticism is expressed by entertaining other models, with a particular interest in ones that are statistically close to the benchmark model. This approach has antecedents in the robust control literature.[3] Formally, solve

$$\min_{\substack{L_{t+\epsilon}\geq 0 \\ \mathbb{E}(L_{t+\epsilon}|\mathfrak{F}_t)=1}} \mathbb{E}\left(L_{t+\epsilon}\widehat{V}_{t+\epsilon} \mid \mathfrak{F}_t\right) + \xi\mathbb{E}\left(L_{t+\epsilon}\log L_{t+\epsilon} \mid \mathfrak{F}_t\right) = -\xi\log\mathbb{E}\left[\exp\left(-\frac{1}{\xi}\widehat{V}_{t+\epsilon}\right) \mid \mathfrak{F}_t\right], \quad 5.$$

which is familiar from applied probability theory. This minimization problem investigates the expected utility consequences of altering the probability distribution subject to a conditional relative entropy penalty used as a Kullback-Leibler measure of statistical divergence. The parameter ξ penalizes the search over alternative probabilities. Setting $\xi = \infty$ implements expected logarithmic utility. Small values of the penalty imply a large aversion to uncertainty about the transition probabilities.

The minimizing solution to the problem in Equation 5 is

$$L^*_{t+\epsilon} = \frac{\exp\left(-\frac{1}{\xi}\widehat{V}_{t+\epsilon}\right)}{\mathbb{E}\left[\exp\left(-\frac{1}{\xi}\widehat{V}_{t+\epsilon}\right)|\mathfrak{F}_t\right]}, \quad 6.$$

provided that the denominator is well-defined. This formulation gives an example of what Maccheroni, Marinacci & Rustichini (2006) call variational preferences designed to confront broader notions of uncertainty other than risk. The minimizing probability displays what is called exponential tilting, as the probabilities are slanted toward more adverse continuation values in an exponential manner. The implied minimizer is also of interest for the reasons articulated by the robust Bayesian, Good (1952), as a way to assess plausibility. Also, the implied measure of statistical divergence is revealing as a measure of statistical challenges implicit in the choice of the penalty parameter ξ.

This construction is an alternative interpretation for the large risk aversion often imposed in recursive utility models. The mathematical equivalence can be seen by letting $\xi = \frac{1}{\gamma-1}$. The economic interpretation, however, is very different—as is the assessment of what are plausible calibrations of the uncertainty adjustment in the utility recursion.

[3] See, for instance, Jacobson (1973), Whittle (1981), James (1992), and Petersen, James & Dupuis (2000).

2.3. Continuous-Time Limit

To depict the continuous-time counterpart to Equation 1, suppose that the continuation utility evolves as[4]

$$d\widehat{V}_t = \hat{\mu}_{v,t}dt + \sigma_{v,t} \cdot dB_t,$$

where $\hat{\mu}_{v,t}$ is the local mean and $|\sigma_{v,t}|^2$ is local variance. In positing this evolution, we are using local normality induced by the Brownian increments to deduce the local normality of the continuation utility increments.

The limiting version of the recursion in Equation 1 gives the following restriction on $(\hat{\mu}_{v,t}, |\sigma_{v,t}|^2)$:

$$0 = \left(\frac{\delta}{1-\rho}\right)\left[(C_t/V_t)^{1-\rho} - 1\right] + \hat{\mu}_{v,t} + \left(\frac{1-\gamma}{2}\right)|\sigma_{v,t}|^2. \tag{7.}$$

For the unitary IES case ($\rho = 1$), Equation 7 becomes

$$0 = \delta\left(\widehat{C}_t - \widehat{V}_t\right) + \hat{\mu}_{v,t} + \left(\frac{1-\gamma}{2}\right)|\sigma_{v,t}|^2. \tag{8.}$$

Equations 7 and 8 provide an expression for the local mean $\hat{\mu}_{v,t}$ as a function of $\widehat{C}_t - \widehat{V}_t$ and the local variance $|\sigma_{v,t}|^2$.[5]

Consider once again the robust interpretation of our recursive preferences and the minimization problem (Equation 5). This problem has a simplified version in the case of a Brownian motion information structure. Let L be a positive martingale or likelihood ratio used to induce an alternative probability distribution. From the Girsanov theorem, under the probability measure induced by L, the process B becomes a Brownian motion with a drift $H \overset{\text{def}}{=} \{H_t : t \geq 0\}$. Locally, the Brownian increment dB_t inherits a drift $H_t dt$. The evolution of L thus takes the form

$$dL_t = L_t H_t \cdot dB_t$$

and, in logarithms,

$$d\widehat{L}_t = -\frac{1}{2}|H_t|^2 dt + H_t \cdot dB_t,$$

with normalization $L_0 = 1$ or equivalently $\widehat{L}_0 = 0$. Under the implied change of probability measure, the drift of $\widehat{L}$ is $-\frac{1}{2}|H_t|^2$, a local measure of Kullback-Leibler divergence or relative entropy. The continuous-time formulation of Equation 5 then becomes

$$\min_{H_t} \hat{\mu}_{v,t} + \sigma_{v,t}H_t + \frac{\xi}{2}|H_t|^2.$$

The minimizing H_t is

$$H_t^* = -\frac{1}{\xi}\sigma_{v,t}', \tag{9.}$$

[4]Starting with V instead of $\widehat{V}$, we would write $dV_t = V_t[\mu_{v,t}dt + \sigma_{v,t} \cdot dB_t]$, where $\hat{\mu}_{v,t} = \mu_{v,t} - \frac{1}{2}|\sigma_{v,t}|^2$.

[5]We find this representation to be pedagogically revealing, with a direct heuristic link to familiar discrete-time specifications. Continuation values are only well-defined up to a strictly increasing transformation as emphasized by Duffie & Epstein (1992). For mathematical reasons, often a different ordinally equivalent representation, $(V_t)^{1-\gamma}/(1-\gamma)$, is used in many papers constructed to remove the volatility contribution to the recursion.

with a minimized objective given by

$$\widehat{\mu}_{v,t} - \frac{1}{2\xi}|\sigma_{v,t}|^2. \tag{10.}$$

The negative of the local exposure vector, $\sigma_{v,t}$, of the continuation value to Brownian risk determines the direction of the drift adjustment to the stochastic state evolution. Comparing this result to the limiting recursion (Equation 7), the parameter γ can be viewed as a form of uncertainty aversion, instead of as a measure of risk aversion, when using $\gamma - 1 = 1/\xi$. Not surprisingly, this agrees with our discrete-time discussion of Section 2.2.

2.4. Stochastic Discount Factor Process

We deduce a representation for the shadow stochastic discount factor (SDF) process in discrete time and continuous time. For economies with a single agent type, this shadow SDF provides a convenient representation of equilibrium asset prices. In heterogeneous agent economies with financing frictions, the shadow SDFs are typically not equalized across agent types but can be used to represent commonly traded assets. Moreover, their differences reflect the absence of full risk-sharing induced by market frictions.

Think of the SDF process S as providing a way to depict shadow prices over any investment horizon. In particular, $S_{t+\epsilon}/S_t$ in conjunction with the transition probabilities associated with an underlying probability measure give date-t prices for a payoff at date $t + \epsilon$. Deduce the shadow SDF process by computing the intertemporal marginal rate of substitution across different possible realized states in the future. By differentiating through the utility recursion, the evolution over a period of length ϵ, expressed in logarithms, is

$$\widehat{S}_{t+\epsilon} - \widehat{S}_t = -\epsilon\delta - \rho\left(\widehat{C}_{t+\epsilon} - \widehat{C}_t\right) + (1-\gamma)\left[\widehat{V}_{t+\epsilon} - \widehat{\mathbb{R}}(\widehat{V}_{t+\epsilon} \mid \mathfrak{F}_t)\right] + (\rho - 1)\left[\widehat{V}_{t+\epsilon} - \widehat{\mathbb{R}}(\widehat{V}_{t+\epsilon} \mid \mathfrak{F}_t)\right].$$

Of particular interest, the term $(1-\gamma)[\widehat{V}_{t+\epsilon} - \widehat{\mathbb{R}}(\widehat{V}_{t+\epsilon} \mid \mathfrak{F}_t)]$ adjusts for risk or robustness. Its exponential has conditional expectation equal to unity and is equal to the minimizer $L^*_{t+\epsilon}$ in Equation 6. Thus, this particular contribution to the SDF induces a change in the probability distribution motivated explicitly by robustness considerations. More generally, the difference between $\widehat{V}_{t+\epsilon}$ and its certainty equivalent $\widehat{R}_t$ is forward-looking and depends on the decision-maker's perspective of the future. This contribution vanishes when $\gamma = \rho$. When $\rho = 1$, only the contribution captured by the change in probability measure is forward-looking.

Next, consider the local evolution of the SDF, written as

$$dS_t = -r_t S_t dt - S_t \pi_t \cdot dB_t.$$

With this representation, r_t is the instantaneous risk-free rate and π_t is the vector of local prices of exposure to the Brownian increment dB_t, also called risk prices. Similarly, write the local consumption evolutions as

$$d\widehat{C}_t = \hat{\mu}_{c,t}dt + \sigma_{c,t} \cdot dB_t.$$

Then, in terms of the dynamics of $\widehat{C}$ and $\widehat{V}$, we have the following riskless rate and risk prices, respectively:

$$r_t = \delta + \rho\hat{\mu}_{c,t} - \frac{1}{2}|\pi_t|^2 + \frac{(\gamma-1)(\gamma-\rho)}{2}|\sigma_{v,t}|^2$$

$$\pi_t = \rho\sigma_{c,t} + (1-\rho)\sigma_{v,t} + (\gamma-1)\sigma_{v,t}.$$

Notice that the third contribution to the risk-price vector is negative of the robustness adjustment, H^*_t, to the drift of the vector Brownian motion, as depicted in Equation 9. The second contribution vanishes when the intertemporal elasticity, $\frac{1}{\rho}$, is unity.

3. LOCAL MEASURES OF EXPOSURES AND PRICES

In all of the models we consider, the logarithms of several quantities of interest will grow or decay stochastically over time with increments that are stationary Markov processes. Let M be such a process and $\widehat{M}$ its logarithm. Restrict the process $\widehat{M}$ to display linear, stochastic growth or decay. We write

$$\widehat{M}_{t+\epsilon} - \widehat{M}_t = \epsilon \hat{\mu}_m(X_t) + \sigma_m(X_t) \cdot (B_{t+\epsilon} - B_t), \tag{11.}$$

where X is an asymptotically stationary Markov process. Examples of such $\widehat{M}$ processes in our models are the log SDF $\widehat{S}$ and log consumption $\widehat{C}$.

3.1. Shock Elasticities

Shock elasticities are constructed using local changes in the exposure to shocks. For instance, consider a shock $B_\epsilon - B_0$ that is distributed as a multivariate standard normal. We introduce a parameterized family of random variables $H_\epsilon(\mathsf{r})$,

$$\log H_\epsilon(\mathsf{r}) = \mathsf{r}\nu(X_0) \cdot (B_\epsilon - B_0) - \frac{\mathsf{r}^2}{2}\epsilon|\nu(X_0)|^2,$$

where we normalize the row vector ν so that $\mathbb{E}\left[|\nu(X_0)|^2\right] = 1$. In our applications, ν is state independent and selects one of the components of $B_\epsilon - B_0$. Notice that $H_\epsilon(\mathsf{r})$ is positive and has conditional expectation equal to one. Consider the following:

$$\frac{d}{d\mathsf{r}} \log \mathbb{E}\left[\left(\frac{M_t}{M_0}\right) H_\epsilon(\mathsf{r}) \mid X_0\right]\Big|_{\mathsf{r}=0} = \frac{\nu(X_0) \cdot \mathbb{E}\left[\left(\frac{M_t}{M_0}\right)(B_\epsilon - B_0) \mid X_0\right]}{\mathbb{E}\left[\left(\frac{M_t}{M_0}\right) \mid X_0\right]}. \tag{12.}$$

We refer to the outcome as a shock elasticity because we differentiate a logarithm with respect to an argument $H_\epsilon(\mathsf{r})$, which is equal to one at $\mathsf{r} = 0$. This elasticity depends on the state X_0 and horizon t. When scaled by $\frac{1}{\epsilon}$, it has a well-defined limit as ϵ declines to zero.

In Equation 12, notice that the essential input is

$$\frac{\mathbb{E}\left[\left(\frac{M_t}{M_0}\right)(B_\epsilon - B_0) \mid X_0\right]}{\epsilon \mathbb{E}\left[\left(\frac{M_t}{M_0}\right) \mid X_0\right]}. \tag{13.}$$

The numerator is a vector of conditional regression coefficients of $\frac{M_t}{M_0}$ onto $B_\epsilon - B_0$, since the regressors have a conditional covariance matrix that scales an identity matrix by ϵ. In the language of empirical macroeconomics, these vectors are conditional counterparts to local projections.[6] The denominator of Formula 13 is included because of our interest in characterization involving M instead of $\widehat{M}$, as is often done by empirical macroeconomists and because we are interested in measuring elasticities. The continuous-time limits can be computed numerically in a straightforward way for the Markovian economies of the type we consider here.[7]

[6]The continuous-time limits are related to constructs from stochastic process theory. The Haussmann-Clark-Ocone formula gives continuous-time moving-average representations of general processes constructed from underlying Brownian motion information structures. The counterparts to moving-average coefficients are stochastic and interpreted as conditional expectations of so-called Malliavin derivatives. The limiting version of the numerator of Formula 13 can be viewed as an approximation to the coefficient on dB_0 in such a representation. These types of computations also play an important role in characterizing derivative claims pricing (see Fournié et al. 1999). For a more complete development and discussion of the connections to various continuous-time representations, see Borovička, Hansen & Scheinkman (2014).

[7]For further discussion, see Borovička, Hansen & Scheinkman (2014).

The scaling by H_ϵ in Equation 12 (or its continuous-time limit) has two distinct interpretations depending on the application:

1. It changes the distribution of B_ϵ by giving it a conditional mean $\epsilon \mathsf{r}\nu(X_0)$.
2. It changes the exposure of $\widehat{M}_t - \widehat{M}_0$, and hence M_t/M_0, to the shock $B_\epsilon - B_0$ through the addition of $\mathsf{r}\nu(X_0) \cdot (B_\epsilon - B_0)$.

The first of these interpretations provides a distributional version of an impulse-response function. It matches exactly for the linear, log-normal model, in which case X is a multivariate, Gaussian vector autoregression—that is, when μ is affine in x, and ν and σ_m are vectors of constants. Once we include nonlinearities, the state x can matter along with the time horizon t.[8] For intertemporal asset-pricing applications, the second interpretation will help us understand shock elasticities as implied compensations for changes in the exposures. We discuss this asset-pricing application next.

3.2. Compensations for Exposure to Uncertainty

Let $\widehat{Y}$ denote the logarithm of a cash flow process and $\widehat{S}$ denote the equilibrium log SDF process, both of which have stochastic evolutions of the form in Equation 11. Compute the following:

1. exposure elasticity,
$$\frac{\nu(X_0) \cdot \mathbb{E}\left[\left(\frac{Y_t}{Y_0}\right)(B_\epsilon - B_0) \mid X_0\right]}{\epsilon \mathbb{E}\left[\left(\frac{Y_t}{Y_0}\right) \mid X_0\right]};$$
2. value elasticity,
$$\frac{\nu(X_0) \cdot \mathbb{E}\left[\left(\frac{S_t Y_t}{S_0 Y_0}\right)(B_\epsilon - B_0) \mid X_0\right]}{\epsilon \mathbb{E}\left[\left(\frac{S_t Y_t}{S_0 Y_0}\right) \mid X_0\right]}; \quad \text{and}$$
3. price elasticity (exposure minus value),
$$\frac{\nu(X_0) \cdot \mathbb{E}\left[\left(\frac{Y_t}{Y_0}\right)(B_\epsilon - B_0) \mid X_0\right]}{\epsilon \mathbb{E}\left[\left(\frac{Y_t}{Y_0}\right) \mid X_0\right]} - \frac{\nu(X_0) \cdot \mathbb{E}\left[\left(\frac{S_t Y_t}{S_0 Y_0}\right)(B_\epsilon - B_0) \mid X_0\right]}{\epsilon \mathbb{E}\left[\left(\frac{S_t Y_t}{S_0 Y_0}\right) \mid X_0\right]}.$$

These all have well-defined continuous-time limits as $\epsilon \downarrow 0$. As mentioned above, one can interpret the price elasticity as the expected excess return required for a marginal increase in risk exposure to Y.

There is one additional calculation of interest. Suppose that $L = \exp(\widehat{M})$ is a martingale. This is of interest when we entertain beliefs that differ from the data-generating process and study their value contribution. From the Law of Iterated Expectations,
$$\frac{\nu(X_0) \cdot \mathbb{E}\left[\left(\frac{L_t}{L_0}\right)(B_\epsilon - B_0) \mid X_0\right]}{\epsilon \mathbb{E}\left[\left(\frac{L_t}{L_0}\right) \mid X_0\right]} = \left(\frac{1}{\epsilon}\right) \nu(X_0) \cdot \mathbb{E}\left[\left(\frac{L_\epsilon}{L_0}\right)(B_\epsilon - B_0) \mid X_0\right]$$
and does not depend on the horizon t. In this circumstance (and perhaps others as well), we find it revealing to change the date of the Brownian increment by reporting the small ϵ limit of
$$\frac{1}{\epsilon}\mathbb{E}\left[\left(\frac{L_t}{L_0}\right)\nu(X_{t-\epsilon}) \cdot (B_t - B_{t-\epsilon}) \mid X_0\right] \tag{14.}$$
as a term structure of uncertainty prices. These prices will be horizon dependent.

[8]For related constructs of nonlinear impulse responses, see Gallant, Rossi & Tauchen (1993) and Koop, Pesaran & Potter (1996).

4. ECONOMIES WITH A REPRESENTATIVE INVESTOR

For pedagogical purposes, we begin our exposition by focusing on a representative investor with recursive preferences in a complete-market production economy featuring long-run risk shocks. We may view the economy as a production-based counterpart to that in the seminal paper by Bansal & Yaron (2004). In part we share a similar ambition to that of Jermann (1998) in describing a production-based model with asset pricing, but we also use this class of models as a benchmark for model classes that include heterogeneous capital or heterogeneous investors. We follow Bansal & Yaron (2004) by focusing on recursive utility—in contrast to the work by Jermann (1998), which features habit persistence preferences.

Since our benchmark model features complete markets, we study the planner problem to characterize equilibrium quantities and prices in the economy. A decentralized version of the model allows for a rich set of assets locally spanning the Brownian increments along with a riskless security. Risk prices are embedded in the SDF evolution.

Even for a model with a single capital stock, the introduction of production and investment turns out to be important relative to endowment economies when we change preference parameters. Much of the asset-pricing literature features endowment economies in which changes in the IES have only a pricing impact. As we illustrate, in a production economy, changing the IES has a substantial impact on the investment-capital ratio and hence growth in the underlying economy.

4.1. Exogenous Stochastic Inputs

We presume that there are two underlying exogenous processes that evolve as solutions to stochastic differential equations:

$$dZ_t^1 = -\beta_1 Z_t^1 dt + \sqrt{Z_t^2}\sigma_1 \cdot dB_t \tag{15.}$$

$$dZ_t^2 = -\beta_2 (Z_t^2 - \mu_2) dt + \sqrt{Z_t^2}\sigma_2 \cdot dB_t, \tag{16.}$$

where $\beta_1 > 0$, $\beta_2 > \frac{1}{2}|\sigma_2|^2$, and $\mu_2 > 0$. In addition, σ_1 and σ_2 are d-dimensional vectors of real numbers. The Z^1 process governs the conditional mean of the stochastic component to technology growth, and the Z^2 process captures the exogenous component to aggregate stochastic volatility. Notice that $\sqrt{Z^2}$ scales the Brownian increment to both of the processes. The local variance of the exogenous technology shifter is $Z_t^2|\sigma_1|^2$, and the local variance for the stochastic volatility process is $Z_t^2|\sigma_2|^2$.

The stochastic variance process Z^2 is a special case of a Feller square root process. The exogenous stochastic technology growth process, Z^1, is a continuous-time version of an autoregression with innovations that are conditionally heteroskedastic. The autoregressive coefficients for discrete-time counterparts are $\exp(-\beta_1)$ and $\exp(-\beta_2)$. Values of β_1 and β_2 that are close to zero imply a large amount of persistence. The unconditional mean of Z^1 is normalized to be zero, and the unconditional mean of Z^2 in a stochastic steady state is μ_2. In what follows, we let

$$Z_t \stackrel{\text{def}}{=} \begin{bmatrix} Z_t^1 \\ Z_t^2 \end{bmatrix}, \qquad \mu_z(Z_t) \stackrel{\text{def}}{=} \begin{bmatrix} -\beta_1 Z_t^1 \\ -\beta_2 (Z_t^2 - \mu_2) \end{bmatrix}, \qquad \text{and} \qquad \sigma_z \stackrel{\text{def}}{=} \sqrt{Z_t^2} \begin{bmatrix} \sigma_1' \\ \sigma_2' \end{bmatrix}.$$

4.2. Technology

We use a so-called AK technology with adjustment costs to represent production.[9] Let K_t be the stock of capital, I_t the investment rate, and C_t the consumption rate at date t. The technology

[9] See, e.g., Cox, Ingersoll & Ross (1985), Merton (1973), Jones & Manuelli (1990), and Brock & Magill (1979).

consists of two equations: an output equation and a capital evolution equation. Output is constrained by

$$C_t + I_t = \alpha K_t, \tag{17.}$$

where α is a fixed productivity parameter. Our capital accumulation equation features aggregate shocks, as follows:

$$dK_t = K_t \left[\Phi\left(\frac{I_t}{K_t}\right) + \beta_k Z_t^1 - \eta_k \right] dt + K_t \sqrt{Z_t^2}\sigma_k \cdot dB_t, \tag{18.}$$

where η_k embeds an adjustment for depreciation and σ_k is a $d \times 1$ vector quantifying the importance of the Brownian motion in generating stochastic returns to investment. The function Φ, called the installation function by Hayashi (1982), is an increasing and concave function. A leading example of Φ in our article is

$$\Phi(i) = \frac{1}{\phi}\log(1 + \phi i), \tag{19.}$$

where i is a stand-in for a realization of the investment-capital ratio. The small i quadratic approximation is

$$\Phi(i) \approx i - \frac{\phi}{2} i^2.$$

We note this relationship since quadratic specifications are often imposed in the investment literature.

By design, the technology is homogeneous of degree one in investment, capital, and consumption. This model has stochastic shocks that (*a*) alter the physical returns to investment; (*b*) shift the conditional mean of that investment; and (*c*) shift the aggregate volatility of the technology. For such a stylized model, capital should be interpreted very broadly and potentially should include human, organizational, and intangible contributions. The shock to physical returns to investment is sometimes referred to as a capital quality shock or a technology shock.[10]

4.3. Value Function

Given the homogeneity properties of both preferences and technology, the value function scales linearly with the capital stock. It will be most convenient to work with the logarithm of the value function, which we posit takes the following form:

$$\widehat{V}_t = \widehat{K}_t + \upsilon(Z_t). \tag{20.}$$

We combine the evolutions of $\upsilon(Z_t)$ and $\widehat{K}_t$ to deduce a Hamilton-Jacobi-Bellman equation for the function υ:

$$\begin{aligned} 0 = \max_{c+i=\alpha} \Bigg\{ & \left(\frac{\delta}{1-\rho}\right)\left(c^{1-\rho}\exp\left[(\rho-1)\upsilon\right] - 1\right) + \Phi(i) + \beta_k z_1 - \eta_k - \frac{1}{2} z_2 |\sigma_k|^2 \\ & + \mu_z \cdot \frac{\partial \upsilon}{\partial z} + \frac{z_2}{2}\text{trace}\left\{\sigma_z{}' \frac{\partial^2 \upsilon}{\partial z \partial z'}\sigma_z\right\} + \frac{(1-\gamma)z_2}{2}\left|\sigma_k + \sigma_z{}' \frac{\partial \upsilon}{\partial z}\right|^2 \Bigg\}, \end{aligned} \tag{21.}$$

[10] Our model is isomorphic to an AK model where productivity (instead of capital K_t) is being hit by Brownian shocks and in which adjustment costs also scale up and down with such shock.

where c is the consumption-capital ratio and i is the investment-capital ratio. The first-order condition for the optimal consumption-capital ratio, ι^*, is

$$\delta\,[\iota^*(z)]^{-\rho}\exp\left[(\rho-1)\upsilon(z)\right]=\Phi'\left[\alpha-\iota^*(z)\right]. \tag{22.}$$

Capital provides the sole source of wealth in this economy. Total wealth is given by the continuation value divided by the marginal utility of consumption, evaluated at equilibrium outcomes:[11]

$$\frac{1}{\delta}\,[\iota^*(z)]^{\rho}\exp[(1-\rho)\upsilon(z)]k.$$

The implied price of capital is given by $Q_t = q(Z_t)$, where

$$q(z)=\frac{1}{\delta}\,[\iota^*(z)]^{\rho}\exp[(1-\rho)\upsilon(z)]=\frac{1}{\Phi'\left[\alpha-\iota^*(z)\right]}=1+\phi i^*(z). \tag{23.}$$

The instantaneous capital return in this economy has an exposure to the vector, dB_t, of Brownian increments given by

$$\sigma_{r,t}=\sqrt{Z_t^2}\sigma_k+\sqrt{Z_t^2}\,\frac{\partial \ln q}{\partial z'}(Z_t)\sigma_z,$$

where the first term captures the exposure of capital to the Brownian increments and the second one reflects the exposure of valuation to these same increments.

4.4. Single-Capital Stock Economies

In contrast to the other economies that we study, this economy can be well approximated by log-quadratic approximations. We use this as a benchmark to the study of economies that are more explicitly nonlinear. We imagine a family of economies indexed by $(\rho, \gamma, \delta, \alpha)$. Of course other parameter sensitivity could also be explored. Our use of a production economy provides a revealing contrast to the familiar Lucas (1978) endowment economy.

In consumption-based models with endowment specifications, the preference parameter ρ has a substantial impact on the risk-free rate. In models with production, like the ones we explore here, changing ρ while holding other parameters of preferences and technology fixed has a substantial impact on production and savings. **Table 1** gives parameter values that we hold fixed in these computations, and **Table 2** reports the steady-state investment-to-output and consumption-output ratios along with the steady-state growth rate. The IES has a dramatic impact on all of these average macroeconomic aggregates.

To diminish this impact, we change the productivity parameter α to pin down a common growth rate in consumption. **Table 3** reports the results. There is still a noticeable impact of ρ on investment-to-output and consumption-output ratios, but the impact is not nearly as dramatic. The subjective discount rate also impacts these steady states by increasing the consumption-output ratios, as also seen in **Table 3**.

We next consider shock-exposure and shock-price elasticities. We focus on the growth-rate shock. The capital evolution shock is also quantitatively important. In contrast, the impact of the stochastic volatility shock is quantitatively small.[12] Stochastic volatility does induce state dependence in the other shock elasticities, as we illustrate in **Figure 3**.

[11] The two recursions in Equation 1 are both homogeneous of degree one. From an infinite-dimensional version of Euler's theorem, the continuation value divided by the marginal utility of consumption is the current period shadow price of current and future consumption, which equals wealth in equilibrium.

[12] The quantitative magnitudes could be amplified by pushing the mean reversion parameter β_2 even closer to zero, as is done in calibrations of asset-pricing models.

Table 1 Parameter values that we hold fixed for the one-capital model[a]

η_k	ϕ	β_k	β_1	β_2	μ_2
0.040	8.000	0.040	0.056	0.194	6.3×10^{-6}
	Upper triangular			**Lowe triangular**	
σ_k	$\sqrt{12}$ [0.92 0.40 0]			$\sqrt{12}$ [1 0 0]	
σ_1	$\sqrt{12}$ [0 5.7 0]			$\sqrt{12}$ [2.3 5.2 0]	
σ_2	$\sqrt{12}$ [0 0 0.00031]				

[a]The numbers for $\eta_k, \phi, \beta_1, \sigma_k$, and σ_1 are such that, when multiplied by stochastic volatility, they match the parameters from Hansen & Sargent (2021). In particular, the constant Z^2, which scales our σ_k to match Hansen & Sargent (2021), is 7.6×10^{-6}. This is the 67th percentile of our Z^2 distribution. While Hansen & Sargent (2021) use a lower triangular representation for the two-by-two right block of $[\sigma_k', \sigma_1']'$, we use an observationally equivalent upper triangular representation for most of the results. Both versions are listed here. Finally, the numbers for β_2 and σ_2 come from Schorfheide, Song & Yaron (2018), but they are adjusted for approximation purposes as described in Appendix A. In both cases, we use the medians of their econometric evidence as input into our analysis.

Table 2 Steady states for alternative specifications of ρ for $\alpha = 0.092$ and $\delta = 0.010$[a]

ρ	**0.67**	**1.00**	**1.50**
Consumption-output ratio	0.012	0.175	0.279
Investment-output ratio	0.988	0.825	0.721
Steady-state growth rate	0.028	0.019	0.013

[a]These are computed by setting shock variances to zero.

Consider the shock-exposure elasticity—or, equivalently, the local impulse-response function—for the investment-output ratio. Since output is proportional to capital, Equation 23 implies these are also approximately the elasticities for the price of capital (which is affine in the investment-capital ratio). As **Figure 1** shows, the responses to a growth-rate shock are positive when $\rho < 1$ and negative when $\rho > 1$. The elasticities are only modestly sensitive to changing the risk-aversion parameter γ, while they increase notably when the subjective discount rate δ is increased.

Table 3 Steady states adjusting the productivity parameter α to match a specific growth rate[a]

	$\delta = 0.010$		
ρ	**0.67**	**1.00**	**1.50**
Consumption-output ratio	0.071	0.175	0.296
Investment-output ratio	0.929	0.825	0.704
Productivity (α)	0.082	0.092	0.108
Growth rate	0.019	0.019	0.019
	$\delta = 0.015$		
ρ	**0.67**	**1.00**	**1.50**
Consumption-output ratio	0.155	0.242	0.346
Investment-output ratio	0.845	0.758	0.654
Productivity (α)	0.090	0.100	0.116
Growth rate	0.019	0.019	0.019

[a]These are computed by setting the shock variances to zero.

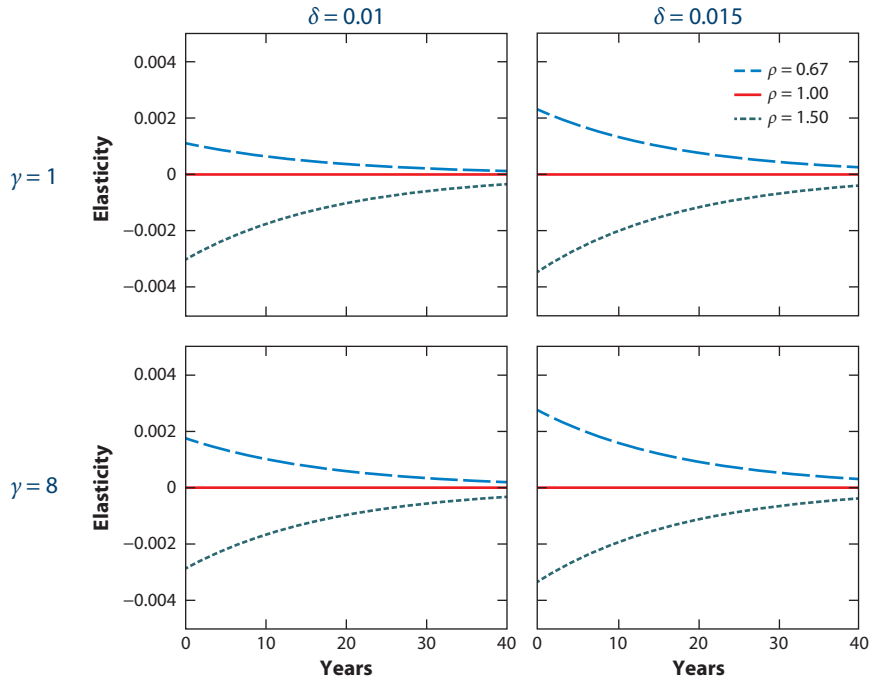

Figure 1

Investment-output ratio exposure elasticities to a growth-rate shock for different values of uncertainty aversion γ and discount rate δ. The growth and volatility states are initialized to their medians.

Finally, we consider both the shock exposure and price elasticities of consumption in **Figure 2**. The consumption elasticity to a growth-rate shock builds over time, as expected given investment adjustment costs. The $\rho = 1$ elasticities imitate those of an endowment economy like the Bansal & Yaron (2004) economy (without stochastic volatility). The risk-aversion parameter γ has very little impact on these exposure elasticities, in contrast to the price elasticities. As revealed by **Figure 2**, the shock-price elasticities are very sensitive, as expected, to the choice of γ. Recall the robustness interpretation of recursive utility, where misspecification concerns contribute a martingale component to valuation. This component comes to dominate as γ becomes larger, which leads to a relatively flat shock-price elasticity trajectory.

Figure 3 shows how the elasticities depend on the initial level of volatility. The key takeaway is that stochastic volatility provides exogenous fluctuations in risk pricing, in contrast to some of the more endogenous mechanisms that we explore going forward. In addition, as is well understood, a shock to exogenous volatility itself is priced under these preferences.

4.5. Endogenous Fluctuations in Valuation

In this section, we illustrate an endogenous channel induced by ambiguity aversion by building on ideas from Chen & Epstein (2002), Hansen (2007), Andrei, Hasler & Jeanneret (2019), and, in particular, Hansen & Sargent (2021). As we show, this channel adds a form of state dependence in valuation. For this illustration, we focus exclusively on the case in which $\rho = 1$. To feature the endogeneity of fluctuations in valuation, we abstract from exogenously specified stochastic

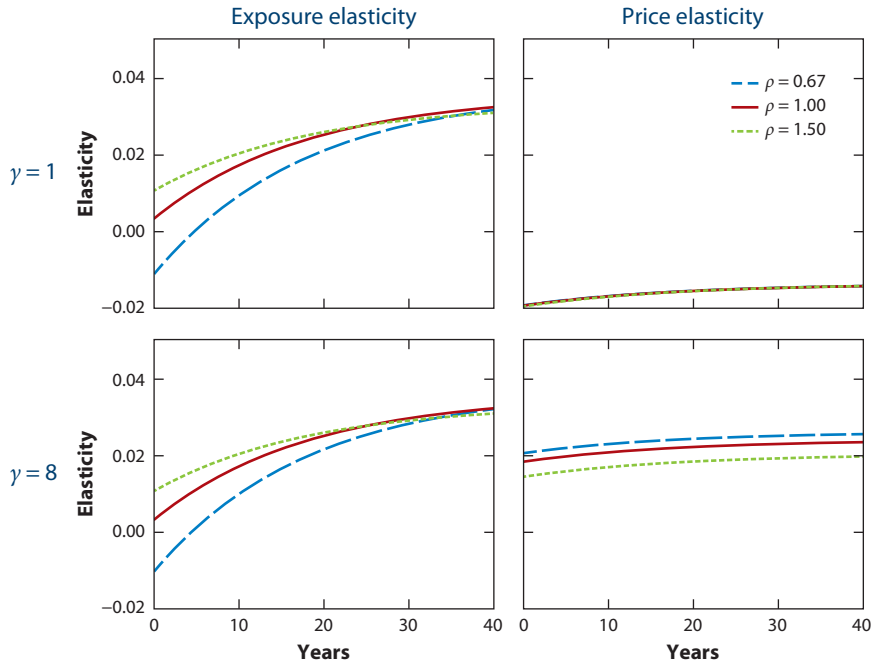

Figure 2

Exposure and price elasticities for the growth-rate shock for different values of uncertainty aversion γ and inverse IES ρ. Perturbations are relative to the equilibrium consumption process. The growth and volatility states are initialized to their medians. Abbreviation: IES, intertemporal elasticity of substitution.

volatility in this subsection (by setting $\sigma_2 = 0$). In addition, we impose that

$$\sigma_k = \begin{bmatrix} 0.0087 & 0.0038 & 0 \end{bmatrix}$$

$$\sigma_1 = \begin{bmatrix} 0 & 0.055 & 0 \end{bmatrix}.$$

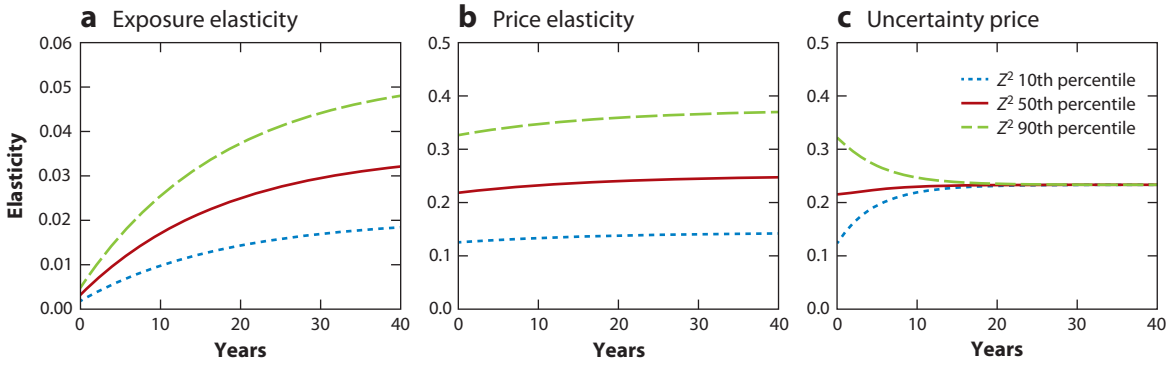

Figure 3

Shock-exposure and shock-price elasticities for uncertainty aversion $\gamma = 8$, inverse IES $\rho = 1$, and alternative volatility Z^2 quantiles. The shock elasticities apply to the growth-rate shock. The growth state is initialized to its median. Abbreviation: IES, intertemporal elasticity of substitution.

We follow Hansen & Sargent (2022) by considering both model ambiguity and potential model misspecification. Recall that recursive utility provides a direct link to the latter, an approach that we continue to use here. For model ambiguity, we proceed differently. Given a parameterized family of models, the investor is unsure how much weight should be given to each. For a Bayesian decision-maker, this would be addressed with subjective inputs in the form of a prior. Our investor is unsure which such prior to impose. Formally, we use a framework for diffusion processes that is consistent with Chen & Epstein (2002) to entertain a rich family of what Hansen & Sargent (2022) refer to as "structured" models.

In our application, we start with a four-dimensional space of unknown parameters in the drifts of capital K and the growth rate Z^1. We modify the evolution of Z^1 to be

$$dZ_t^1 = \left(\psi_1 - \beta_1 Z_t^1\right) dt + \sigma_1 \cdot dB_t,$$

where the parameter ψ_1, which we have taken to be zero so far, allows for a shift in the local drift dynamics that does not scale with Z^1. In the long-term, $\psi_1 \neq 0$ could induce a nonzero unconditional mean in Z^1 process. The unknown parameters are η_k, β_k, ψ_1, and β_1. Recall that η_k governs depreciation and β_k governs the exposure to long-term growth-rate uncertainty. Our investors take uncertainty in these parameters as a starting point, but they entertain a so-called time-varying parameter perspective without imposing a prior on the form of the time variation. Instead, the parameters are constrained to be in an ambiguity set using a recursive measure of relative entropy or Kullback-Leibler divergence as described by Hansen & Sargent (2021).

We consider two specifications. One limits the ambiguity to be over the two slope parameters, β_k and β_1, and the other also includes the constant terms, η_k and ψ_1. **Figure 4** plots both the two-dimensional and four-dimensional ambiguity sets. By construction, the projection of the slope coefficients for the four-dimensional set is contained within the two-dimensional ambiguity

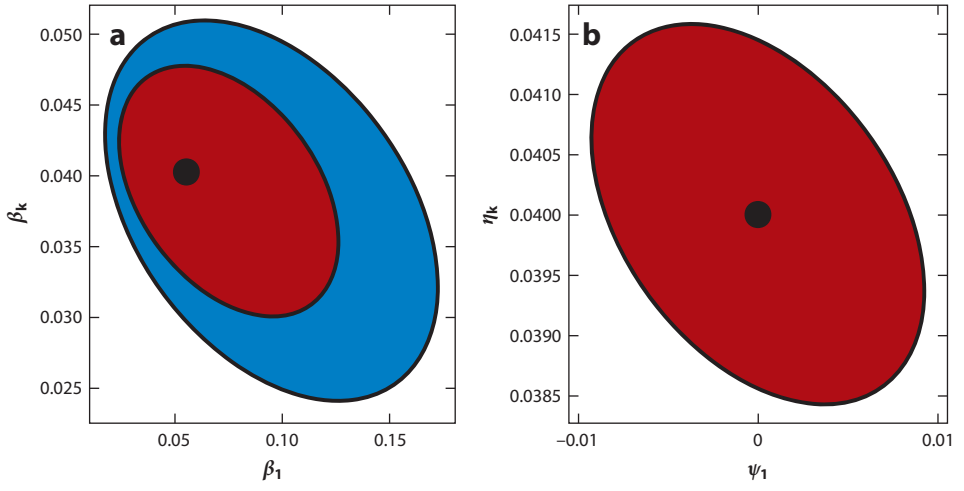

Figure 4

Ambiguity parameter sets constrained by a flow measure of relative entropy developed by Hansen & Sargent (2021). Panel *a* depicts the ambiguity in the slope coefficients β_k and β_1 for the state Z_t^1 in the capital evolution and the state evolution, respectively. The blue region plots a two-dimensional ambiguity set, and the red region gives the two-dimensional projection for the four-dimensional ambiguity set. The red region in panel *b* gives the two-dimensional projection of the constant terms η_k and ψ_1 in the capital and state evolution, respectively, for the four-parameter ambiguity set. Baseline values for the four parameters are recorded as black dots.

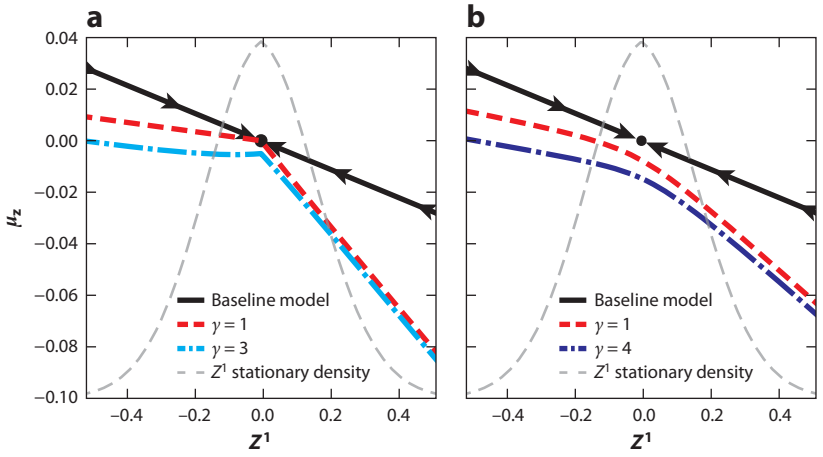

Figure 5

Uncertainty-adjusted growth-rate drift μ_z and baseline stationary density for stochastic growth Z^1. The black solid line illustrates the baseline drift, while the red and blue curves are the uncertainty-adjusted nonlinear counterparts. The dot-dashed curves include misspecification concerns in addition to parameter ambiguity. Panel *a* shows implications when the ambiguity consideration is limited to the slope coefficients, while panel *b* illustrates outcomes when the ambiguity is four-dimensional. The lower value of uncertainty aversion γ in panel *a* relative to panel *b* is imposed so that the magnitudes of the misspecification adjustments are approximately the same. The gray dashed curve depicts the stationary density for Z^1. The black arrows indicate that there is reversion toward the mean at zero.

set as depicted in **Figure 4*a***.[13] By design, this approach entertains misspecification relative to a benchmark in a much more structured way than that embedded in the robust interpretation of the Kreps & Porteus (1978) utility.

Recall that in the standard continuous-time recursive formulation of dynamic programming, the decision-maker maximizes the expected value-function increment by choice of a control. In our recursive formulation of ambiguity, a fictitious second agent algorithmically minimizes the expected value-function increment over the respective sets of parameter values, instant-by-instant. The minimizer will reside somewhere on the boundary, and its location will depend on the realized growth-rate state, z^1. The problem is made tractable in part because the minimization problem is quadratic. We also include potential model misspecification in the same manner as described previously. As we have shown, $\gamma = 1$ abstracts from misspecification concerns, while larger values of γ enhance these concerns.

We illustrate the nonlinear outcome by reporting the implied uncertainty-adjusted (minimizing) drift for the long-run growth process in **Figure 5**. The downward slope of the line in the baseline model governs the pull toward zero in the conditional mean dynamics for Z^1. The figure includes curves that incorporate uncertainty adjustments. It also contains results when the ambiguity concerns are limited to the slope coefficients.

Observe that these curves are flatter for negative growth rates and steeper for positive growth rates. This is to be expected because investors fear persistence when growth is sluggish and the lack of persistence when growth is brisk. This outcome emerges in the computations in part because of how the minimizing choice of β_1 over the ambiguity set displayed in **Figure 4** depends on Z^1. The

[13] We constructed these sets using, in the notation of Hansen & Sargent (2021), $q = 0.2$ with $\rho_1 = 0$ and $\rho_2 = \frac{q^2}{|\sigma_1|^2}$ for the two-parameter case, and $\rho_2 = \frac{q^2}{2|\sigma_1|^2}$ for the four-parameter case.

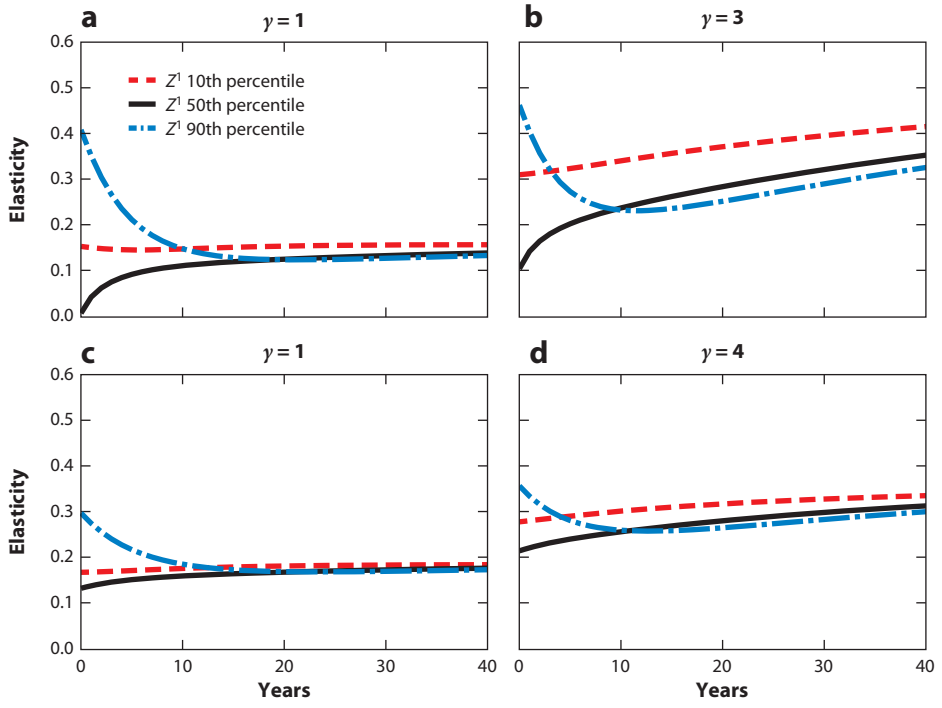

Figure 6

Shock-price elasticities for the martingale contribution induced by uncertainty aversion. The figure shows the median of the Z^1 stationary distribution (*black solid line*), 10th percentile (*red dashed line*), and 90th percentile (*blue dot-dashed line*). The top row gives results for uncertainty aversions (*a*) $\gamma = 1$ and (*b*) $\gamma = 3$ when the ambiguity set is two-dimensional. The bottom row gives results for (*c*) $\gamma = 1$ and (*d*) $\gamma = 4$ for the four-dimensional ambiguity set.

investor is exploring the other parameters as well, and the outcome of minimization also impacts a counterpart for drift specification for capital.

While the one-capital model without ambiguity concerns can be approximately solved using log-quadratic specification, the model with ambiguity requires a global alternative to capture the potential nonlinearities that are entertained by the decision-maker.

The two forms of uncertainty aversion we consider introduce a composite martingale component to valuation. We explore its properties by looking at the implied uncertainty price elasticities using Formula 14. The results are reported in **Figure 6**. We represent state dependence by exploring not only the median but also the 10th and 90th percentiles. While the 90th percentile prices start higher than the others, this is reversed as we go out to longer horizons. This pattern reflects the decrease in persistence in the uncertainty-adjusted probability measure for relatively high realized values of the growth state Z_t^1. As is evident from **Figure 6*b*,*d***, misspecification concerns contribute to the asymmetry in the responses in an important way. This is particularly true for the two-dimensional specification of ambiguity aversion.

In summary, we induce changes in asset values by investors' altering their perspectives on what models are most concerning within the constrained ambiguity set. These fluctuations prevail in large part because of uncertainty in the persistence of the process Z^1. In low-growth states, investors are concerned about being stuck in a rut, whereas in good times, they worry that brisk growth will end soon. This type of mechanism was noted by Hansen (2007) in a distinct but

related modeling framework. That paper uses a different specification of ambiguity aversion and entertains explicit learning. In the example here, learning is off the table because of potential time or state variation in parameters. Relatedly, learning about persistence was also featured by Andrei, Hasler & Jeanneret (2019) as a mechanism for fluctuations over time in valuation.

4.6. Sluggish Heterogeneous Capital Stocks

We now explore two-capital models with growth-rate uncertainty. Precursors of these models are the multiple-tree models of Cochrane, Longstaff & Santa-Clara (2008) and Martin (2013). These models do not entertain capital movements from one production source to another. Here, we follow Eberly & Wang (2009, 2011), Hansen et al. (2020), and Kozak (2022) by allowing capital mobility subject to adjustment costs. In this sense, capital movements are sluggish. We extend the capital evolution in Eberly & Wang (2009, 2011) and Kozak (2022) by introducing exposures to an exogenously specified growth-rate uncertainty consistent with our previous examples, similar to Hansen et al. (2020). We allow for the exposure to this uncertainty to be heterogeneous.

Formally, consider a family of models with two capital stocks and adjustment costs:

$$dK_t^j = K_t^j \left[\Phi^j \left(\frac{I_t^j}{K_t^j} \right) + \beta_k^j Z_t^1 - \eta^j \right] dt + K_t^j \sqrt{Z_t^2} \sigma_k^j \cdot dB_t,$$

for $j = 1, 2$. Suppose that the output equation is now

$$C_t + I_t^1 + I_t^2 = \alpha K_t^a,$$

where aggregate capital is a CES aggregator of the two capital stocks:

$$K_t^a = \left[(1-\zeta) \left(K_t^1 \right)^{(1-\tau)} + \zeta \left(K_t^2 \right)^{(1-\tau)} \right]^{\frac{1}{1-\tau}},$$

for $0 \leq \zeta < 1$ and $\tau \geq 0$. For characterization and computation, we form two state variables: One is $\widehat{Y}_t = \log(K_t^2 / K_t^1)$, and the other is $\widehat{K}_t^a$. For this class of models, the value function has the separable form:

$$\widehat{V}_t = \widehat{K}_t^a + \upsilon(\widehat{Y}_t, Z_t).$$

Eberly & Wang (2009, 2011), Hansen et al. (2020), and Kozak (2022) feature the case in which the two capital stocks are perfect substitutes ($\tau = 0$, $\zeta = 0.5$). In the figures that follow, we also impose this restriction as a featured special case. Our computational software allows for production curvature among the two capital stocks, and as we will illustrate, this opens the door to an even richer collection of examples. With perfect substitutability, the deterministic limit of this model has a continuum of steady states. This makes locally linear-quadratic approximations inoperative. Even with production curvature, local methods can be unreliable. Thus, we find global solutions' approaches to be important for this class of examples.

The parameter values that we use in this section are recorded in **Table 4**. We consider two different specifications of the exposures. One specification is symmetric. While each capital stock has its own shock, the relative importance of long-term uncertainty to each K^j is the same. The other specification is asymmetric. The first capital stock is not exposed to long-run uncertainty, while the second one is. **Table 4** gives some additional explanations and details. For these economies, we abstract from parameter ambiguity.

We start by reporting stationary densities in **Figure 7** for the fraction of the capital that is allocated to the second technology. Initially, consider the case of symmetric exposures. We see some sensitivity to the IES with the plots for $\rho = 0.67$ being more peaked. As Eberly & Wang (2011) emphasize, increasing risk aversion through changing γ (or increasing the concern for

Table 4 Parameter values for the two-capital model[a]

Parameters common across the two capitals				
η_k	ϕ	α, ρ	β_1 β_2	σ_1, σ_2
0.040	8.00	$\alpha = 0.16$ 0.18 0.22 $\rho = 0.67$ 1.00 1.50	0.056 0.194	$\sigma_1 = \sqrt{12}[0\ \ 0\ \ 5.7\ \ 0]$ $\sigma_2 = \sqrt{12}[0\ \ 0\ \ 0\ \ 0.00031]$
Symmetric		**Asymmetric**		**Capital volatilities**
$\beta_k^1 = 0.04$		$\beta_k^1 = 0$		$\sigma_k^1 = \sqrt{12}\left[\sqrt{2}\,(0.92)\ \ 0\ \ 0.40\ \ 0\right]$
$\beta_k^2 = 0.04$		$\beta_k^2 = 0.08$		$\sigma_k^2 = \sqrt{12}\left[0\ \ \sqrt{2}\,(0.92)\ \ 0.40\ \ 0\right]$

[a]We include a separate capital shock for each technology. The coefficients on the two capital shocks are given by the first two entries of σs. We doubled α for the two-capital model because K_t^a is the average capital stock for each of the three specifications of ρ. To maintain comparability with the single-capital model, we scale the first two entries of σ_k^1 and σ_k^2 by $\sqrt{2}$, since a fictitious social planner can now diversify across the two capital shocks. The specification "symmetric" presumes symmetric exposure to growth uncertainty, while the specification "asymmetric" presumes that only the second capital stock is exposed to growth uncertainty.

misspecification) makes diversification all the more attractive, giving rise to densities that are much more sharply peaked. It is noteworthy that when $\gamma = 1$ the asymmetric parameterization flattens out the allocation densities. But, arguably more interesting, when $\gamma = 8$ the second capital stock becomes much less attractive and even more so as we decrease ρ. The mode of the density is now centered near .2 instead of .5 as investors seek to avoid exposure to long-term uncertainty. For the model specifications discussed so far, the two capital stocks are perfect substitutes in the production of output.

So far, the only heterogeneity in the capital stock is in the exposure to shocks and long-term uncertainty. We next illustrate the impact of production function curvature by making the elasticity of substitution across the two types of capital one ($\tau = 1$) and one-half ($\tau = 2$). (See the bottom row of **Figure 7**.) This decrease in elasticity of substitution in production makes the stationary densities more peaked. This is to be expected given the more central role played by both capital stocks in the production of output. We include this computation as an illustration only, as there are alternative substantive motivations for multiple capital stocks with differential impacts on production. For example, intangible, organizational, and human capital contribute to production in arguably distinct ways. While incorporation of these components could lead to even richer models, the force on display in **Figure 7** will still be present.[14]

Figure 8 plots the shock elasticities or local impulse responses for the aggregate investment-capital ratio. We only depict these for $\gamma = 8$, as the $\gamma = 1$ responses are very similar. The elasticities for the symmetric case are very similar to those we computed for the one-capital model. In contrast, the responses in the asymmetric case are more muted, consistent with the flatter densities reported in **Figure 7**. **Figure 9** depicts the shock-price elasticities for the growth shock. We report only the case in which $\gamma = 8$, as the $\gamma = 1$ results are unsurprisingly small. The price elasticities are very flat, reflecting a dominant martingale component to the SDF. Recall that we used robustness concerns to model misspecification as an important contributor to this martingale. The magnitude of the growth-rate shock-price elasticities is very close to those we reported for the single-capital model. In the asymmetric case, the prices are significantly smaller because capital is reallocated to reduce the exposure to growth-rate uncertainty.

[14]For a recent discussion of modeling and measuring intangible capital, see Crouzet et al. (2022).

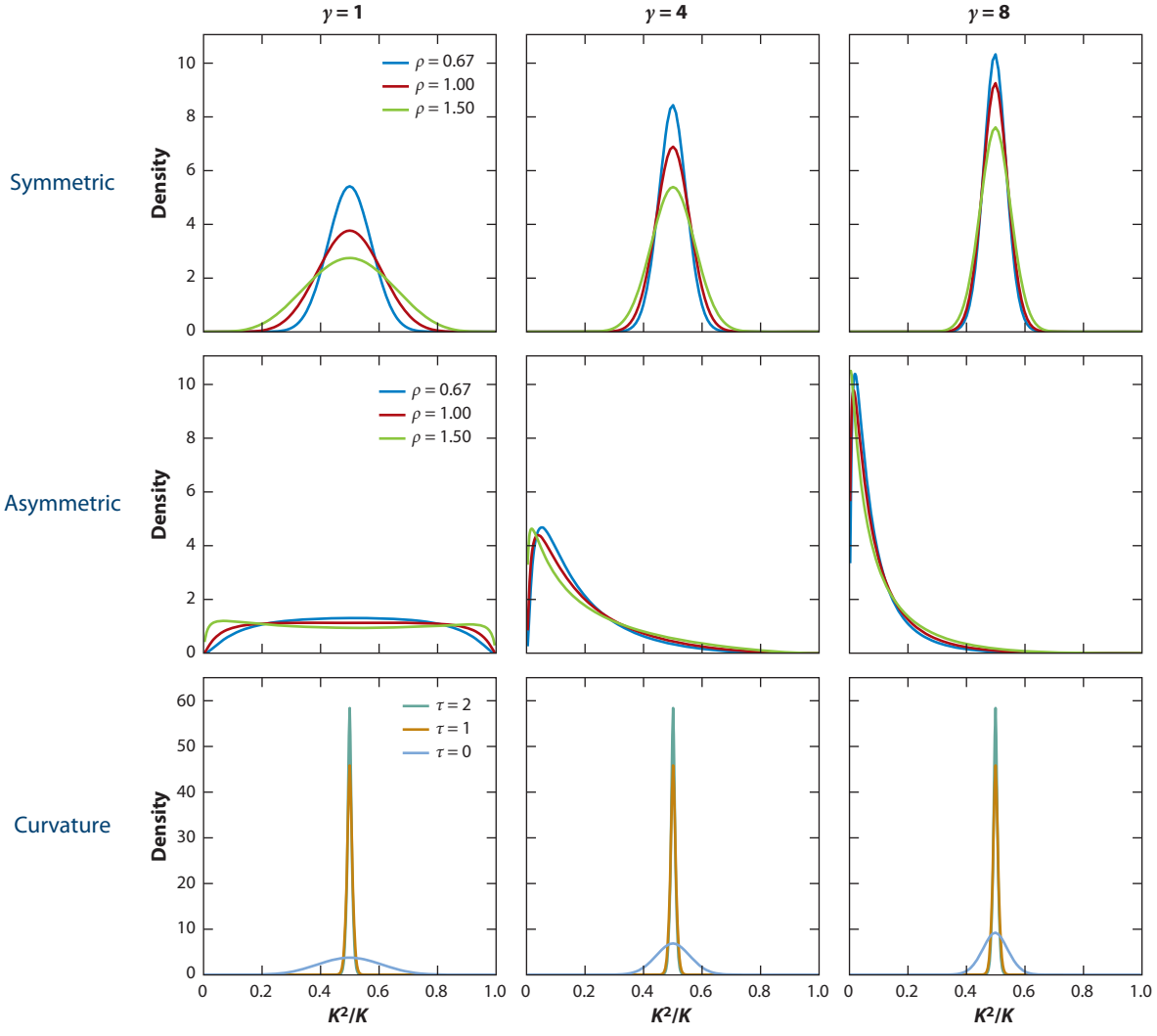

Figure 7

Stationary densities for the second capital stock K^2 as share of total capital K, where τ is the elasticity of substitution between the two types of capital. For the symmetric row (*top row*), both capital stocks are exposed to the same growth-rate uncertainty. For the asymmetric row (*middle row*), only the second capital stock is exposed to growth-rate uncertainty. For the curvature row (*bottom row*), the $\tau = 1$ specification assumes a unitary substitution elasticity across the two types of capital, and the $\tau = 2$ specification assumes a substitution elasticity equal to 1/2. The results in the bottom row impose inverse IES $\rho = 1$ and the same exposure to long-term uncertainty for both capital stocks. Abbreviation: IES, intertemporal elasticity of substitution.

5. HETEROGENEOUS AGENTS AND FINANCIAL FRICTIONS

We now explore a different form of heterogeneity. We alter our one-capital baseline model in Section 4 to include (ex ante) agent heterogeneity and financial frictions. Agents will be heterogeneous in their preferences, productivities, and financial market access. We think of the baseline economy as one in which multiple economic agents have homogeneous preferences and homogeneous access to the production technology. In this case, consumption and wealth are proportional over time, making aggregation immediate. This simple aggregation will not be true in the class of

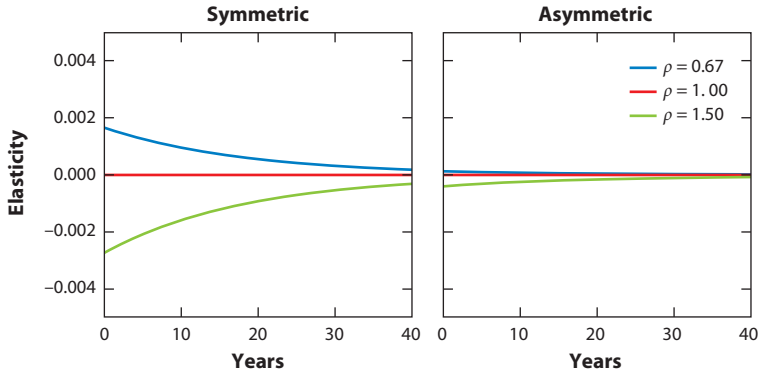

Figure 8

Investment-output ratio exposure elasticities for growth-rate shock for uncertainty aversion $\gamma = 8$ across different values of inverse IES ρ. The state variables are initialized at their medians. Abbreviation: IES, intertemporal elasticity of substitution.

economies that we explore in this section. With various forms of market impediments, we can no longer focus on the planner problem as has been true in our previous examples. Instead, we study a competitive equilibrium in which wealth heterogeneity matters. As in our previous economies, we entertain the possibility of growth-rate uncertainty in the production technology. We feature model comparisons within a conveniently nested class of models.

5.1. Environment, Equilibrium, and Solution Overview

There are two agent types in the economy: experts and households, indexed by e and h, respectively. Both agents have recursive preferences, but their preference parameters (δ, γ, ρ) can differ. There is a single capital accumulation technology, but the productivity of this capital stock may differ in the hands of each of the agents, with $\alpha_e \geq \alpha_h$. Capital trades freely among agents, with price Q_t that follows endogenous diffusive dynamics.

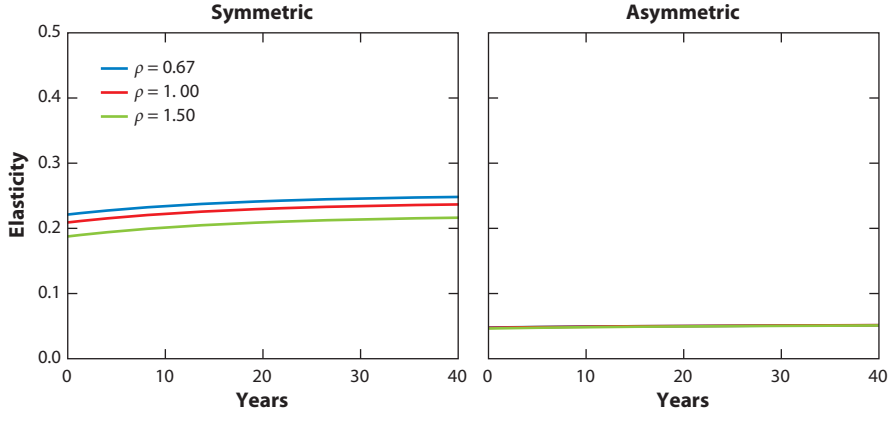

Figure 9

Consumption price elasticities for the growth-rate shock for uncertainty aversion $\gamma = 8$ across different values of inverse IES ρ. The state variables are initialized at their medians. Abbreviation: IES, intertemporal elasticity of substitution.

Several financial instruments also trade risk-free short-term debt at an interest rate r_t, and various financial claims are exposed to aggregate risk: (*a*) derivatives contracts traded among households at vector π_t per unit of Brownian increment risk exposure; and (*b*) equity contracts issued by experts with payoff proportional to the return on capital they hold. In some of our economies, experts face a financial restriction: They must remain exposed to at least a fraction $\underline{\chi}$ of the total capital they hold. Experts, therefore, cannot issue unlimited equity nor can they trade freely in hedging contracts.

Let N_t^j be the date-t net worth of type-j agent for $j = b, e$. Then,

$$\frac{dN_t^j}{N_t^j} = \left(\mu_{n,t}^j - C_t^j/N_t^j\right) dt + \sigma_{n,t}^j \cdot dB_t, \tag{24.}$$

where the local mean $\mu_{n,t}^j$ net of consumption and the shock-exposure vector $\sigma_{n,t}^j$ are

$$\mu_{n,t}^j = r_t + \frac{Q_t K_t^j}{N_t^j}\left[\mu_{R,t}^j - r_t\right] + \theta_t^j \cdot \pi_t \qquad \text{and} \qquad \sigma_{n,t}^j = \frac{Q_t K_t^j}{N_t^j}\sigma_{R,t} + \theta_t^j$$

and where K_t^j and θ_t^j denote the capital and hedging positions chosen by the type-j agent. A hedging position θ_t^j implies an exposure $N_t^j \theta_t^j \cdot dB_t$ to Brownian risk. As capital is also exposed to Brownian risk, $\sigma_{n,t}^j$ reflects both exposures. Due to productivity differences, the expected excess return on capital $\mu_{R,t}^j - r_t$ is type-specific (see the online **Supplemental Appendix B** for the expression for $\mu_{R,t}^j$). The risk exposure vector for capital, $\sigma_{R,t}$, is common for households and experts and has a direct contribution from capital-quality shocks and a contribution from the market price Q_t of capital.

Supplemental Material >

Market incompleteness is encoded via a constraint on the hedging vector θ_t^e of experts. While households are unconstrained, experts have restrictions on their exposure to aggregate risk. Suppose experts choose θ_t^e to reduce their exposure to capital risk by a fraction χ_t. To achieve this reduction,

$$\theta_t^e = (\chi_t - 1)\frac{Q_t K_t^e}{N_t^e}\sigma_{R,t}.$$

Imposing a so-called skin-in-the-game constraint, $\chi_t \geq \underline{\chi}$ restricts the ability of the experts to hedge their risk to the capital that they own:

$$\theta_t^e \in \left\{(\chi_t - 1)\frac{Q_t K_t^e}{N_t^e}\sigma_{R,t} \quad : \quad \chi_t \geq \underline{\chi}\right\}. \tag{25.}$$

Notice that even in the limit, relaxing this constraint still limits the type of hedging that can be done by experts, since the portfolio weights remain constrained to be proportional to $\sigma_{R,t}$. For the purpose of making model comparisons, the structure just described embeds three types of heterogeneity. First, there is preference heterogeneity. In addition to heterogeneous subjective discounting, we allow for $\gamma_b \geq \gamma_e$, which can reflect either an enhanced aversion to risk on the part of households or less confidence in the probability model. Second, we allow for experts to use capital more productively than households ($\alpha_e \geq \alpha_b$). Finally, we entertain heterogeneity in financial market access: the skin-in-the-game restriction in Equation 25 limits experts' abilities to offset their capital risk exposure via equity issuance. These alternative forms of heterogeneity allow revealing comparisons across alternative model specifications.

Our definition of a competitive equilibrium is standard: It is a set of price processes (Q, π, r) and allocation processes $(C^e, C^b, N^e, N^b, K^e, K^b, \chi, \theta^e, \theta^b)$, such that agents solve their constrained optimization problems, taking price processes as given, and all markets—the goods market, the market for capital, and the market for derivatives (which are in zero net supply)—clear. By Walras's law, the risk-free debt market will also clear.

We look for a Markovian equilibrium in which the state variables are the wealth distribution, the aggregate stock of capital, as well as the driving processes Z^1, Z^2. Given the homogeneity properties of our model, (*a*) the wealth distribution can be summarized by the experts' wealth share $W_t \stackrel{\text{def}}{=} N_t^e / \left(N_t^e + N_t^b\right)$ and (*b*) all growing processes scale with K_t, which means that $X_t' \stackrel{\text{def}}{=} \left(W_t, Z_t^1, Z_t^2\right)$ can serve as a state vector for our economy. While (Z^1, Z^2) are specified exogenously, the wealth share W evolves endogenously.

The log continuation value of each type-*j* agent takes the additively separable form, analogous to the value function for a benchmark economy given by Equation 20:

$$\widehat{V}_t^j = \widehat{N}_t^j + \upsilon^j(X_t),$$

where $\widehat{N}^j = \log N^j$. We construct a Hamilton-Jacobi-Bellman equation analogous to that given in Equation 21 for the social planner in the benchmark economy. (For these Hamilton-Jacobi-Bellman equations, see online **Supplemental Appendix B**.) The homogeneity properties of our model allow us to derive agents' optimal consumption and portfolio choices as a function of υ^j. For instance, the optimal consumption-wealth ratio for each agent type is

Supplemental Material >

$$c^j(x) = \delta^{1/\rho} \exp\left[(1 - 1/\rho)\upsilon^j(x)\right],$$

and their portfolio choice solves a familiar problem that includes both a mean-variance and a hedging component:

$$\max_{K^j, \theta^j} \left\{ \underbrace{\mu_n^j - \frac{1}{2}\gamma_j |\sigma_n^j|^2}_{\text{mean-variance}} + \underbrace{(1 - \gamma_j)(\sigma_x \sigma_n^j) \cdot \frac{\partial \upsilon^j}{\partial x}}_{\text{hedging}} \right\}. \qquad 26.$$

The outcome of this portfolio problem is a set of Euler equations (when constraints are nonbinding) and inequalities (when constraints are binding). For instance, households will hold strictly positive amounts of capital if and only if their expected excess return $\mu_{R,t}^b - r_t$ is sufficiently high to match the market compensation they could otherwise obtain through derivatives markets. Similarly, experts have an incentive to issue as much equity as possible (and their financial constraint will then bind) when their expected return on capital $\mu_{R,t}^e - r_t$ is greater than the market compensation $\pi_t \cdot \sigma_{R,t}$ they need to pay to holders of their equity. Their issuance constraint does not bind otherwise. Since experts are more productive than households, it is efficient for them to hold all the capital in the economy and exhaust their equity-issuance capacity. In fact, one can show that whenever households hold positive amounts of capital, experts' equity issuance constraint must be binding.

The consumption and portfolio choices of the various agent types lead to endogenous dynamics for the experts' wealth share W_t; its drift rate depends on the consumption-wealth ratio of households relative to that of experts, on experts' leverage and their expected excess return on capital relative to its required market compensation, and on the differential aggregate risk exposure between households and experts. The diffusion coefficient of W_t only depends on this latter force. The wealth share dynamics depend on asset prices, which themselves depend on wealth share dynamics—generating a two-way feedback loop that amplifies capital return volatility (Brunnermeier & Sannikov 2014). While this section only provides an overview of the model solution, its full details are contained in the online **Supplemental Appendix B**.

The remainder of this section explores this heterogeneous agent model in a series of model comparisons, offering some general takeaways. In Section 5.2, we specify four different economic environments that differ in terms of market opportunities and productivities of the two agent

types. In Section 5.3, we explore parameter sensitivity within each of these environments to help elucidate the economic forces at work. And in Section 5.4, we make comparisons across environments by discussing outcomes that both unite and distinguish these models. Finally, we provide some discussion of the extant literature in Section 5.5.

5.2. Alternative Economic Environments

We explore four different types of economic environments. These are motivated by some prior contributions, but they differ in the actual modeling inputs, including a stochastic technology that includes long-run risk. The first environment is motivated by the Basak & Cuoco (1998) model (specification RF for risk-free) in which households can only engage in risk-free exchange in security markets in an environment extended to include long-term uncertainty. Production is done by experts. The second setup allows for unrestricted trade in the equity market, but this remains a partial risk-sharing environment (specification PR) since our model accommodates a three-dimensional specification of the Brownian motion. In the case of only a single shock, our risk-sharing limitation becomes inconsequential, making this setup very similar to that of Dumas, Uppal & Wang (2000) and Gârleanu & Panageas (2015).[15] Our third setup adds a skin-in-the-game constraint on the productive experts along the lines of He & Krishnamurthy (2013), enforced by setting $0 < \underline{\chi} < 1$ on the productive experts (specification SG for skin-in-the-game). Finally, motivated by Brunnermeier & Sannikov (2014), we also allow households to be productive—but less so than experts (specification IP for inefficient production). Here, experts do not trade equity claims (so the SG constraint is maximally tight). The specifications for these four environments are summarized in **Table 5**.

In the reported examples, $\rho_h = \rho_e = 1$ and $\delta_h = .01$. Furthermore, experts will always be less patient than households, in order to accommodate a stationary wealth distribution. Sensitivity to these choices is also interesting and straightforward to explore. When we explore sensitivity to γ_e, we shall refer to this as expert risk aversion, but as we have argued previously, this could equivalently be interpreted as a lack of confidence in the stochastic specification. Specifically, when $\gamma_e < \gamma_h$, experts are more confident in the stochastic specifications of technology than households.

Table 5 Parameter settings for the four different economic environments[a]

Economy	Pneumonic	Household productivity	Market access	Risk aversion
RF	Risk-free	$\alpha_h = -\infty$	$\underline{\chi} = 1$	$\gamma_e \leq \gamma_h$
PR	Partial risk-sharing	$\alpha_h = -\infty$	$\underline{\chi} = 0$	$\gamma_e \leq \gamma_h$
SG	Skin-in-the-game	$\alpha_h = -\infty$	$0 < \underline{\chi} < 1$	$\gamma_e \leq \gamma_h$
IP	Inefficient production	$-\infty < \alpha_h < \alpha_e$	$\underline{\chi} = 1$	$\gamma_e = \gamma_h$

[a]We use the capital accumulation parameters and the parameters governing the exogenous stochastic dynamics given in **Table 1**.

[15]Gârleanu & Panageas (2015) impose exponentially distributed death probabilities in conjunction with an exogenous allocation of agent types at birth. The finite life feature enhances the subjective discounting and pulls the expert wealth fraction toward a prespecified level interpreted as the wealth fraction of experts at birth. For an elaboration, see appendix D of Gârleanu & Panageas (2015). Under our reinterpretation of risk aversion, the death probabilities are known with full confidence, in contrast to the uncertainty induced by the vector Brownian motion. By design, this finite life feature ensures a stationary wealth distribution. In the reported examples we do not impose this finite-life aspect, although our computer code and the full model details in **Supplemental Appendix B** accommodate it.

Supplemental Material >

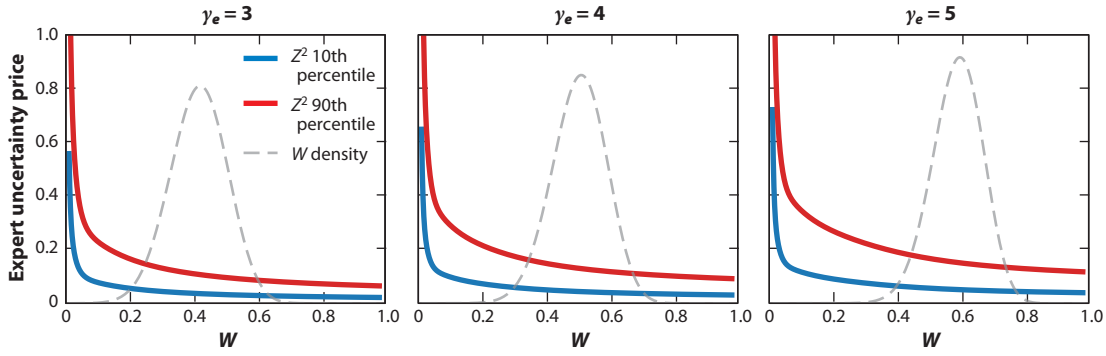

Figure 10

Equity return uncertainty prices for the experts in an environment with only risk-free (RF) financial securities. The prices are expressed as functions of the relative wealth of experts for alternative specifications of expert uncertainty aversion. Household uncertainty aversion is set at $\gamma_b = 8$. The subjective discount rates are $\delta_e = 0.0115$ and $\delta_b = 0.01$. The gray dashed lines represent stationary densities for the expert wealth. For the plots, $Z^1 = 0$ and Z^2 is set to either the 10th percentile (*blue line*) or the 90th percentile (*red line*).

5.3. Comparisons Within Each Economic Environment

We explore the implications of altering the expert risk aversion or the household productivity through four economic environments. Heterogeneity in risk preferences and productivity are two of the key channels to modulate risk price dynamics in this class of models.

5.3.1. Environment RF. We first consider an economic environment in which experts and households only trade a risk-free (RF) asset. We explore the pricing implications of the shadow price for return on capital shocks $\sigma_R \cdot dB$. This is the risk price that would clear a stock market populated only by experts. The results are reported in **Figure 10**. A key force in all the models we explore is the importance of expert wealth: When w falls, risk prices rise, potentially dramatically.[16] In this particular environment, experts must directly absorb all risks, and so their demand for risk compensation rises when w falls. The effect of γ_e depicts a tension between the level and variability of risk prices. When we increase γ_e, we see an upward shift in risk price levels; at the same time, the state dependence in these prices is pushed further into the left tail of the stationary distribution. Intuitively, experts accumulate more wealth for precautionary reasons as γ_e increases. (These plots hold fixed household risk aversion $\gamma_b = 8$, but there is little sensitivity to this choice because households can only trade in an RF security market.) In this environment and the following ones, stochastic volatility contributes importantly to the risk compensations, as is evident by comparing the 10th and 90th percentiles of Z^2 in **Figure 10**.

5.3.2. Environment PR. We next consider an environment in which there is frictionless trading in the equity claim. In this case, we explore implications for both the equity risk price and the equity retention by the experts. The results of this partial risk-sharing (PR) environment are displayed in **Figure 11**. Given that households now have access to equity, its risk price has very limited sensitivity to γ_e. In contrast, the stationary density for experts' relative wealth is sensitive to γ_e. For instance, wealth is very concentrated at zero when $\gamma_e = 5$. Indeed, as γ_e approaches γ_b, the only prominent heterogeneity remaining is from experts' higher consumption rates due to their larger subjective discounting, $\delta_e > \delta_b$, which tends to erode experts' relative wealth.

[16] For a derivation of this countercyclical risk price property in a class of one-shock heterogeneous agent models, see section 2.3 of Panageas (2020).

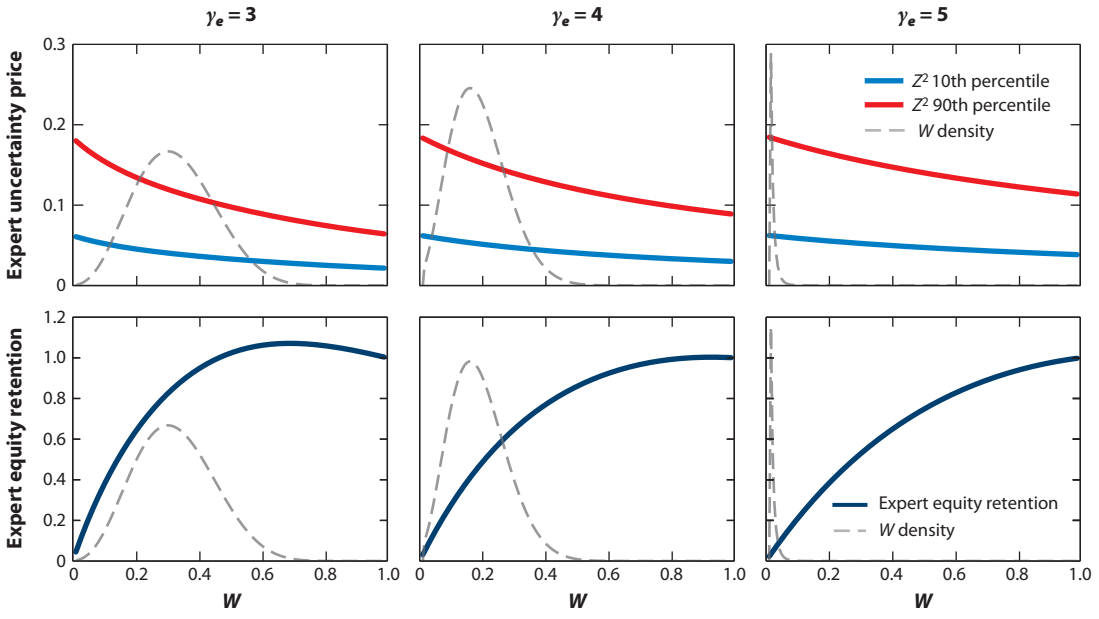

Figure 11

Equity return uncertainty prices (*top row*) and expert equity retention (*bottom row*) for a partial risk-sharing (PR) environment. The objects of interest are expressed as functions of the relative wealth of experts for alternative specifications of expert uncertainty aversion γ_e. Household uncertainty aversion is set at $\gamma_h = 8$. The subjective discount rates are $\delta_e = 0.0115$ and $\delta_h = 0.01$. The gray dashed lines represent stationary densities for the expert wealth share. The axis of the stationary density for $\gamma_e = 5$ is scaled down 17 times relative to $\gamma_e = 3, 4$. For the plots, $Z^1 = 0$ and Z^2 is set to either the 10th percentile (*light blue lines*) or the 90th percentile (*red lines*). The equity retention is not sensitive to changes in stochastic volatility.

With the homothetic preferences we feature, risk-taking is typically monotonic in wealth, because absolute risk aversion is decreasing with wealth. In contrast to this conventional result, **Figure 11** shows that, particularly when γ_e is small relative to γ_h, the equity retention χ by experts is not monotonic in their relative wealth. Moreover, χ exceeds one for some values of w, more prominently when γ_e is particularly small. Why does this occur?

In this PR environment, risk-sharing is limited, and the two agents only trade equity returns. A key force at play in the equity retention figures is households' desire to hedge long-term uncertainty induced by stochastic growth Z^1. Since we have imposed a unitary IES, the Brownian exposure of the return on equity is $\sigma_{R,t} = \sqrt{Z_t^2}\sigma_k$ in this environment. The composite shock $\sigma_k \cdot dB_t$ not only has a direct contribution to the stochastic evolution of capital dK_t but also alters the long-term growth prospects through dZ_t^1 (i.e., growth and capital-quality shocks are correlated). Households, being more risk averse than experts, are more concerned about this growth uncertainty. Absent integrated hedging markets, households use capital to obtain partial insurance against growth-rate fluctuations from experts, leading them to short expert equity for some realizations of the relative wealth share.[17] This same mechanism plays a central role in the determination of a nondegenerate stationary distribution for W. Typically, complete-market models

[17] As further confirmation of this mechanism, unreported results for $\gamma_e = 2$ and $\gamma_h = 8$ show that households' shadow risk prices for exposure to the growth-rate shock range between 0.25 and 0.31 when evaluated at the medians of the exogenous state variables, whereas experts' shadow growth risk price ranges between 0.09 and 0.15. Risk-aversion heterogeneity is critical to this discrepancy in growth risk prices.

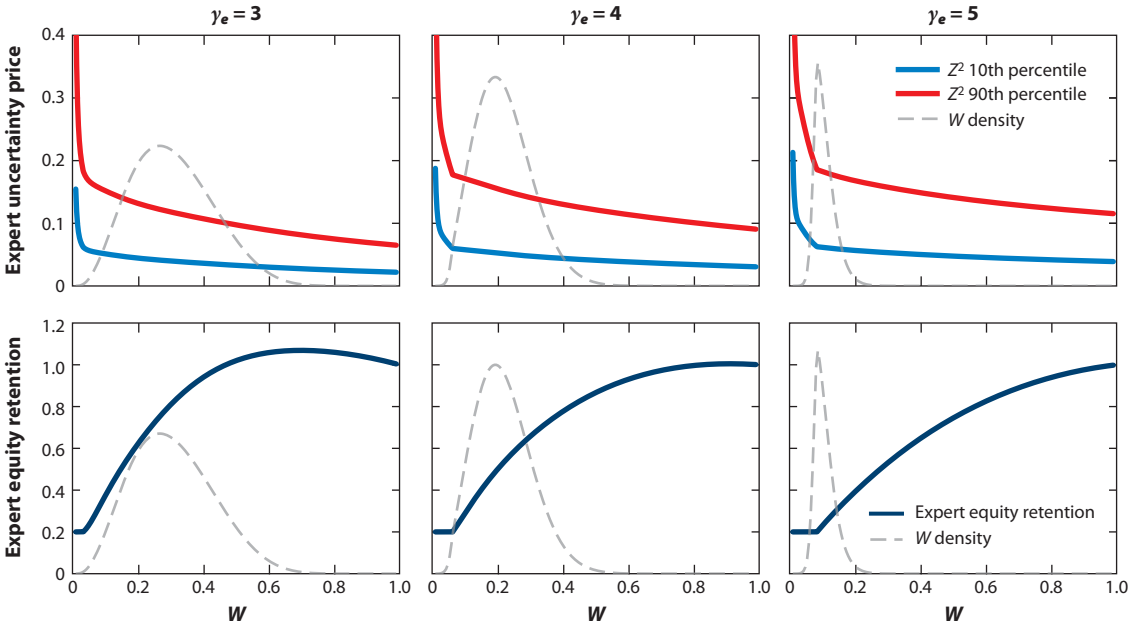

Figure 12

Expert equity return uncertainty prices (*top row*) and expert equity retention (*bottom row*) for a skin-in-the-game (SG) environment. The objects of interest are expressed as functions of the relative wealth of experts for alternative specifications of expert uncertainty aversion γ_e. Household uncertainty aversion is set at $\gamma_h = 8$. The subjective discount rates are $\delta_e = 0.0115$ and $\delta_h = 0.01$. The gray dashed lines represent stationary densities for the expert wealth share. The axis of the stationary density for $\gamma_e = 5$ is scaled down three times relative to $\gamma_e = 3, 4$. For the plots, $Z^1 = 0$ and Z^2 is set to either the 10th percentile (*light blue lines*) or the 90th percentile (*red lines*).

with heterogeneous preferences would, except in knife-edge cases, feature degenerate stationary distributions at $w = 0$ or $w = 1$; here, a broad range of preference parameters can produce nondegenerate wealth distributions.[18]

5.3.3. Environment SG. We next explore the impact of adding a skin-in-the-game (SG) constraint requiring $\chi \geq \underline{\chi} = 0.2$. This constraint binds for low values of the expert wealth share and is occasionally binding in dynamic simulations. We report results in **Figure 12**. Increasing γ_e expands the region in which the constraint binds. **Figure 12** also illustrates the connection between the binding equity constraint and the nonlinear dependence of experts' equity risk price on w; this extreme nonlinearity is why researchers sometimes refer to binding equity constraints as financial crises.[19]

The occasionally binding phenomenon on display in **Figure 12** arises because less-averse experts retain more risk than their wealth (i.e., $\chi > w$), so the unconstrained region remains

[18]We include the dependence between the direct shock to the capital evolution and the shock to exogenous changes in growth-rate opportunities in our examples because of the empirical calibration reported by Hansen & Sargent (2022). Absent this correlation, χ is monotone, increasing in the expert wealth share, and the stationary distribution becomes a point mass at either $w = 0$ or $w = 1$ (depending on the parameters δ_e, δ_h, γ_e, γ_h).

[19]Note that, in this environment, the potentially binding constraint implies we must distinguish experts' and households' shadow risk prices for equity exposure. When $\chi > \underline{\chi}$, the two agree, but when $\chi = \underline{\chi}$, the two diverge. We are plotting experts' shadow risk price.

stochastic (in the sense that $\sigma_w \neq 0$ even when $\chi > \underline{\chi}$). This is essentially what drives the occasionally binding equilibrium of He & Krishnamurthy (2013): They restrict households to always invest a fixed positive fraction of their wealth in risk-free assets, which makes them act more risk averse than experts (see their parameter assumption 1). In fact, we prove for a very general set of cases that the SG constraint is either always binding or never binding when risk aversions are equalized. In this sense, heterogeneous risk preferences are critical to occasionally binding SG constraints.[20]

On one hand, our results here provide a partial justification for the procedure, performed by many DSGE models with financial frictions, that consists in log-linearizing equilibrium equations assuming constraints are always binding. On the other hand, this exercise illustrates that some models with occasionally binding risk-sharing constraints may be standing on (perhaps hidden) assumptions about risk-aversion heterogeneity.

5.3.4. Environment IP. Finally, we explore an environment in which households sometimes engage in production even though experts are more skilled at it (i.e., inefficient production, IP). To isolate the role of productive heterogeneity, we eliminate risk-aversion heterogeneity here. In financial markets, households and experts trade in a risk-free security, but there is no trade in equities as enforced by setting $\underline{\chi} = 1$. When both agents manage capital, however, they face the same exposure to stochastic capital evolution along with growth-rate risk. For computational reasons, we eliminate stochastic volatility for this environment and set Z^2 equal to the mean, μ_2, under the stationary distribution.

In **Figure 13**, we plot experts' shadow capital risk price and their capital share. For low values of the wealth share, households are active producers even though they have lower productivity. In this region, experts demand high shadow compensations for exposure to capital evolution uncertainty. Increasing household productivity increases the likelihood of inefficient household production but decreases the shadow risk price conditional on inefficiency.

5.4. Comparisons Across Environments

In this subsection, we note some interesting comparisons that emerge when we look across environments. Of course, such comparisons may well be sensitive to particular parameter configurations. Our computational methods allow for more comprehensive comparisons done in thoughtful ways.

5.4.1. Deleveraging. Among the four economic environments, we distinguish those that allow deleveraging from those that do not—this demarcation represents a significant divide in the nature of model dynamics.

To explore deleveraging, we consider how the risk share of experts behaves relative to their wealth share. The expert risk share is given by the product $\chi\kappa$, where χ is equity retention fraction and κ is the fraction of capital held by experts. We think of deleveraging occurring when $\chi\kappa$ falls. This is a reasonable definition to consider, since $\chi\kappa$ falling entails experts either selling capital or issuing additional equity.[21]

By this definition, environments RF and SG do not allow deleveraging. In both cases, all capital is held by experts ($\kappa = 1$) and a financial constraint prevents χ from ever falling to zero. Thus,

[20] For analysis of the case when $\gamma_e = \gamma_b$, see online **Supplemental Appendix B** (Proposition B.3). For a large set of parameters, either $\chi_t = \underline{\chi}$ for all t or $\chi_t > \underline{\chi}$ for all t, almost surely.

[21] In all models that we explore, it is true that expert leverage rises as their wealth falls. However, we refer to deleveraging as the *active* decision to reduce risk exposure ($\chi\kappa$) given leverage has risen. Thus, the models that we dub "deleveraging" will have more muted leverage dynamics.

Supplemental Material >

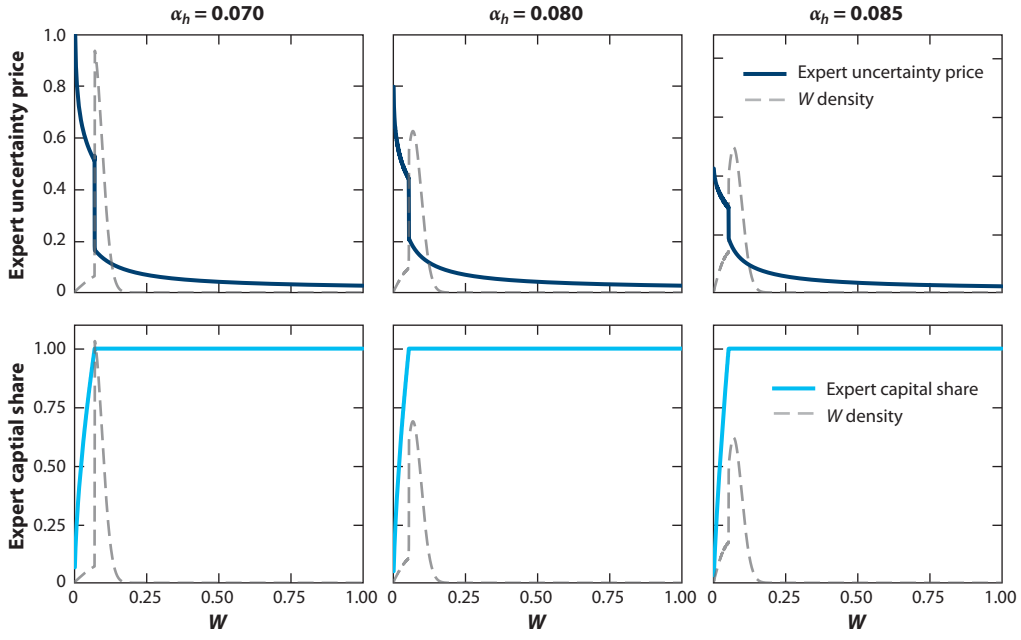

Figure 13

Expert uncertainty prices (*top row*) and expert capital share for an inefficient production (IP) environment. The objects of interest (*blue lines*) are expressed as functions of the relative wealth of experts W. Household and expert uncertainty aversions are the same, $\gamma_h = \gamma_e = 2$. The subjective discount rates are $\delta_e = 0.03$ and $\delta_h = 0.01$. The gray dashed lines represent stationary densities for the expert wealth share. For the plots, $Z^1 = 0$.

$\chi\kappa$ is bounded away from zero for RF and SG. This feature implies that as the wealth share of experts declines to zero, experts' risk exposure per unit of their wealth grows without bound, which in turn implies experts require unbounded risk compensation as $w \to 0$ (see **Figures 10** and **12**). High-risk prices allow experts to earn high profits and recapitalize their balance sheets.

Environments PR and IP do allow deleveraging. In PR, while all capital is held by experts ($\kappa = 1$), there is no constraint on equity issuance (so χ can fall). In IP, experts can deleverage by directly selling capital to households (so κ can fall). Whether through χ or κ, these two environments feature $\chi\kappa$ tending to zero at the same rate as $w \to 0$. Due to deleveraging, experts' risk prices remain bounded even as $w \to 0$ (see **Figures 11** and **13**).

Supplemental Material >

Supplemental Appendix B (Section B.10) conducts a formal asymptotic analysis as $w \to 0$. We show analytically how the deleveraging behavior of $\chi\kappa$, through its effect on equilibrium risk compensations, governs the tail shape of the stationary wealth distribution. Looking back at **Figures 10–13**, one can see how the models with deleveraging can permit substantially more mass near $w = 0$.

5.4.2. Relative wealth dynamics. In **Figure 14**, we report the elasticities for experts' wealth share W_t to an initial capital exposure shock. We document the differential nature of the responses depending on the initial relative wealth position, which demonstrates a form of nonlinearity. With the exception of environment IP, the responses are very flat, suggesting that the shocks have a very persistent impact on the wealth distribution. When we condition on the median wealth share, the responses are lower than when we initialize W_0 at lower percentiles. This is evidence of some

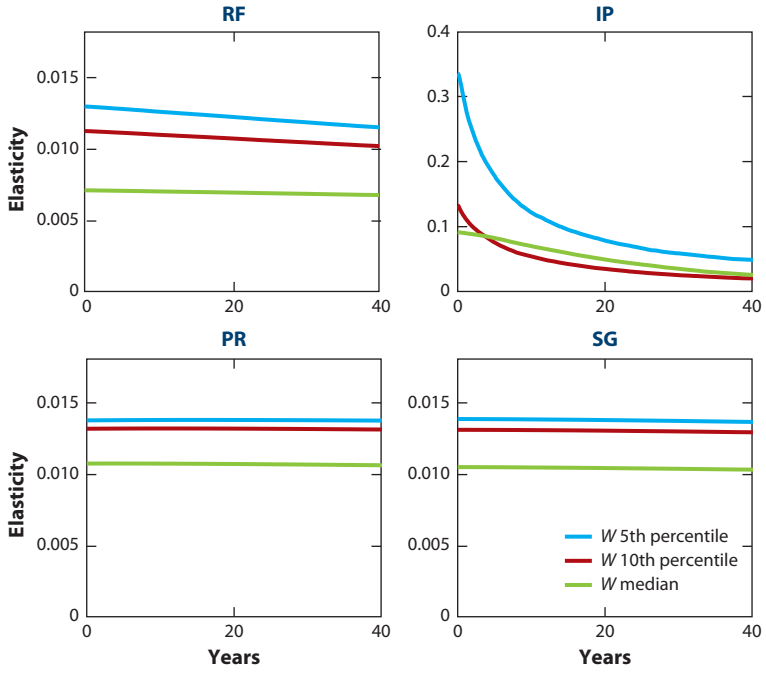

Figure 14

Relative wealth response elasticities to an initial period of capital shock for the four environments. We use expert uncertainty $\gamma_e = 4$ and subjective discount rate $\delta_e = 0.0115$ for environments RF, PR, and SG. For environment IP, we set $\gamma_e = 2$, $\delta_e = 0.03$, and household productivity $\alpha_h = 0.08$. For all environments, household uncertainty aversion $\gamma_h = 8$ and household subjective discount rate $\delta_h = 0.01$. We restrict the initial exogenous state variables to be at their medians. The figure shows elasticities when W is initialized at the 5th percentile (*blue lines*), the 10th percentile (*red lines*), and the median (*green lines*) of the relative wealth distribution. Abbreviations: IP, inefficient production; PR, partial risk-sharing; RF, risk-free; SG, skin-in-the-game.

reversion in these nonlinear settings, since escapes become more likely with enhanced volatility. Initializing at even smaller quantities than we report will reveal more decay in the elasticities, as there will eventually be repulsion from the $w = 0$ boundary.[22]

Recall that, in environments RF and IP, households only trade in risk-free securities. In environment IP, however, households obtain risk exposure from directly holding capital, in contrast to environment RF. As is evident from the top row of **Figure 14**, the shock responses are initially much larger with notable reversion to zero for the IP environment than for the others. This decay in the shock elasticities to zero, as we increase the horizon, is much more substantial for the low quantiles than for the median of the relative expert share of the wealth distribution.

5.4.3. Uncertainty prices. Households and experts share risk in environments PR and SG, but they do not engage in full risk-sharing. Thus, we expect differences in the implied shadow prices for experts and households. Recall that these uncertainty prices use the interpretation of recursive

[22]The finite-life imposition as described in footnote 12 would provide an additional mechanism for reversion away from the boundaries of the wealth distribution.

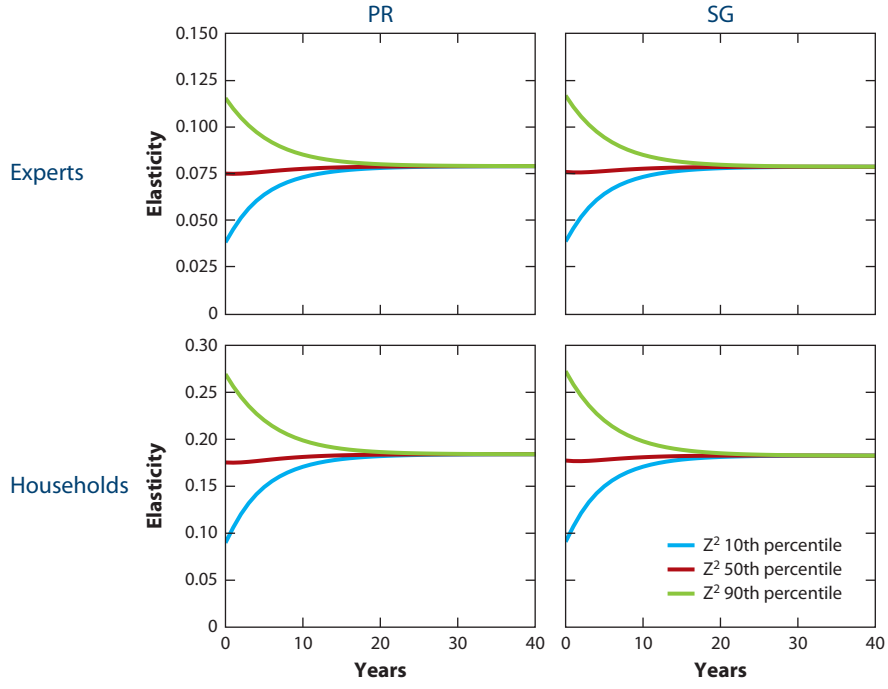

Figure 15

Uncertainty price elasticities for a growth-rate shock for partial risk-sharing (PR) and skin-in-the-game (SG) environments. We use uncertainty aversions $\gamma_e = 4$ and $\gamma_b = 8$ for both models. We initialize W and Z^1 at their medians. The figures show elasticities when Z^2 is initialized at the 10th percentile (*blue lines*), the median (*red lines*), and the 90th percentile (*green lines*) of its distribution.

preferences as an aversion to model misspecification.[23] **Figure 15** explores differences in the implied uncertainty shadow prices for growth-rate shocks for the two agent types. First of all, we see sizable shadow compensation for exposure to growth-rate uncertainty. Second, the significant difference between experts' and households' shadow prices reflects the preference inequality $\gamma_b > \gamma_e$ along with the incomplete risk-sharing. Third, by looking at the differences within each of the four panels, we see the impact of the initial stochastic volatility. And finally, while the shadow price differences are very different between households and experts, the differences across environments are quite modest.[24]

[23] In environments like RF and SG, limited expert deleveraging creates an asymptote for local risk pricing at $w = 0$. While the shadow SDFs play a role in representing intertemporal budget constraints, they may only determine what Hugonnier (2012) refers to as fundamental prices. Since equilibrium wealths are constrained to be positive at all dates, Hugonnier's (2012) insightful paper notes the possibility of bubbles, i.e., equilibrium security prices above their fundamental values. He characterizes the bubbles in terms of local martingales that fail to be global martingales in the SDF processes. From a numerical perspective, this can potentially create subtle issues in computing shock-price elasticities that need to be examined on a case-by-case basis, including the proper treatment of boundary conditions. That being said, this subsection studies the uncertainty prices to growth-rate shocks, as opposed to shocks hitting the level of capital. Since local uncertainty prices for these shocks do not feature such an asymptote at $w = 0$, we conjecture such local martingale issues are not critical to the calculations here.

[24] We found little sensitivity of the uncertainty price shock to the initial wealth share for these calculations.

5.5. Discussion of Related Literature

The models we have explored in this section highlight the role of ex ante agent heterogeneity and risk-sharing. The literature studying this class of models is voluminous, and we do not attempt to survey all of it here. However, we will comment briefly on which existing mechanisms we have covered and which we have not, along with what we see as the challenges for future research in this area.

As mentioned above, the models closest to ours include those by Basak & Cuoco (1998), He & Krishnamurthy (2011, 2013, 2019), Brunnermeier & Sannikov (2014, 2016), and Gârleanu & Panageas (2015). All of these are models where pricing dynamics become interesting either because risk-sharing is constrained or because of the trading dynamics induced by attempts to share risks. Our framework essentially nests these models, pairing them with a setup that features long-run uncertainty in the macroeconomic growth.

These core frameworks have been extended to think about a variety of substantive issues. While our framework does not nest these extensions, we collect some of them here to illustrate the wide range of possibilities: capital requirements and leverage restrictions (Klimenko et al. 2016, Phelan 2016); margin constraints (Gromb & Vayanos 2002, Gârleanu & Pedersen 2011); shadow banking (Moreira & Savov 2017); liquidity premia and monetary policy (Drechsler, Savov & Schnabl 2018); unconventional monetary policy (Silva 2016); international capital flows (Brunnermeier & Sannikov 2015); the link between idiosyncratic and aggregate risk-sharing (Di Tella 2017, 2019); financial innovation–driven boom–bust cycles (Khorrami 2020); and entry into the intermediation sector (Haddad 2014, Khorrami 2021). While we work in continuous time, related issues have been explored in discrete-time frameworks (Gertler & Kiyotaki 2010; Mendoza 2010; Bianchi 2011; Gertler & Karadi 2011; Christiano, Motto & Rostagno 2014; Gertler & Kiyotaki 2015).

While this class of models is rich enough to feature some interesting insights, there are reasons to expand their scope. First, financial crises are often more sudden and extreme than the models we explore here would predict. Second, large booms in credit and asset prices have some predictive power for a subsequent bust and financial crisis. Modeling additional amplification mechanisms like bank runs is one way to generate more realistically extreme crises (Mendo 2018, Krishnamurthy & Li 2021). Modeling investor sentiment, via both nonrational beliefs (Krishnamurthy & Li 2021, Maxted 2024) and rational fear (Khorrami & Mendo 2023), are extensions that can generate crisis predictability.

As an intriguing analogy to our long-run uncertainty framework, Maxted (2024) considers extrapolative sentiment as the belief in a persistent stochastic growth rate that, in fact, does not exist. We could capture such impacts in our framework by supposing that the state variable Z^1 is only in the heads of the investors and households and not in the actual dynamic evolution. We can analyze such a model in the same manner as we currently do by including the Z^1 dynamics in the model solution but omitting it from the simulations, stationary distributions, and elasticity computations. In this way, there is a wedge between beliefs and the actual data generation. We find this alternative perspective on long-term risk to be intriguing, but as we have seen in Section 4.5, an alternative to subjective belief models are ones that acknowledge the measurement challenge of identifying a long-run risk component in data. This challenge seems pertinent to not only econometricians but also economic agents.[25]

The class of models we explored, by design, nests alternative forms of heterogeneity, albeit a rather stark form with two types of investors. For all of the alternatives we investigate, a natural question is, "Who are the so-called experts?" Should we identify them as insiders at productive

[25] For related discussions, see Hansen (2014) and Chen, Dou & Kogan (2024).

firms, managers of banks, or specialist investors more broadly? The answers to these questions influence the type of market frictions that are reasonable to consider as well as the calibrations one should adopt.

One related empirical literature explores intermediary asset-pricing implications by seeking to identify new pricing factors. Models of the type featured here, when applied to financial intermediaries, highlight forms of state dependence in valuation that could be important. Exposures and market compensations fluctuate as functions of state variables, suggesting a more dynamic approach to empirical investigation.

6. CONCLUSIONS

Our article explores alternative macrofinance models, including many with explicit nonlinearities. The models are highly stylized and perhaps best thought of as devices to engage in "quantitative story telling." The models are not designed to provide fully comprehensive accounting of empirical facts; rather, they offer characterizations of alternative mechanisms for linkages between financial markets and the macroeconomy. We feature model comparisons rather than deep probes into one specific mechanism. While the latter is clearly valuable, we also believe in the value of making model comparisons, something that is less common in journal publication. In effect, we are engaged in "quantitative story telling with multiple stories." In this sense, we share a common ambition with Dou et al. (2020), although the class of models we feature and the tools we use are different. Related ambitions are also reflected in the comprehensive Macro Model Data Base (**https://www.macromodelbase.com**), although many of the models we entertain require special computational challenges because of their nonlinear structure. Moreover, our review focuses on the substantive comparisons.

Supplemental Material >

Computational methods are required to support this type of analyses. As we explain in our online **Supplemental Appendix C**, this is a nontrivial component to our investigation.[26] In each model, we must solve for agents' continuation values, in some cases jointly with asset prices or endogenous risk-sharing constraints. These functions solve systems of highly nonlinear PDEs. Depending on the model, we use either finite-difference-based methods or, for larger state spaces, a deep Galerkin method–policy improvement algorithm, incorporating neural net approximations. For some additional macro applications of implicit finite-difference schemes for PDEs, based on the seminal work of Barles & Souganidis (1991), see Achdou et al. (2022) and d'Avernas, Petersen & Vandeweyer (2022). For recent developments and discussions of deep neural network methods as an alternative designed to accommodate higher dimensional state spaces, see Al-Aradi et al. (2022), Duarte, Duarte & Silva (2023), Gopalakrishna (2022), and Barnett et al. (2023).

7. APPENDIX A: STOCHASTIC VOLATILITY CALIBRATION

Recall the volatility process:

$$dZ_t^2 = -\beta_2(Z_t^2 - \mu_z^2) + \sqrt{Z_t^2}\sigma_2 dB_t.$$

Remember that Z^2 has a stationary gamma distribution. Construct the corresponding stationary density for $\widehat{Z}^2 \stackrel{\text{def}}{=} \log Z^2$ using the change of variables formula. Denote the outcome as

$$\hat{q}(\hat{z}; \mu_z^2, |\sigma_2|^2).$$

[26] See also the GitHub repository at **https://github.com/lphansen/comparing_dsge**.

Schorfheide, Song & Yaron (2018) estimate a process for the counterpart to this process with a different stochastic specification. Their process expressed in logarithms is

$$\log \widehat{Z}_t^2 = 2\log \varsigma + H_t^2,$$

where

$$dH_t^2 = -\beta_2 H_t^2 dt + 2\hat{\sigma}_2 dB_t.$$

In table 3 of their paper, they provide estimates based on both a postwar and a longer historical time series. The coefficient β_2 is very similar, but their estimate of $|\hat{\sigma}_2|$ is much larger for the longer time series. We take the following numbers from their table 3 and input into our calibration of stochastic volatility:

$$\beta_2 = \log .984$$

$$|\hat{\sigma}_2| = 2 \times \sqrt{.0054}$$

$$\varsigma = .0022,$$

where the time units are months. The stationary distribution for the Schorfheide, Song & Yaron (2018) model for $\widehat{Z}$ is normal with mean $2\log \varsigma$ and variance

$$\frac{|\hat{\sigma}_2|^2}{2\beta_2}.$$

We denote the distribution as q.

To use the Schorfheide, Song & Yaron estimates for our analysis, we approximate the stationary densities by solving numerically:

$$\min_{\mu_z^2, |\sigma_2|^2} \int_{\hat{z}} \left[\log \hat{q}(\hat{z}; \mu_z^2, |\sigma_2|^2) - \log q(\hat{z})\right] \hat{q}(\hat{z}; \mu_z^2, |\sigma_2|^2) d\hat{z}.$$

The resulting minimizers are

$$\mu_z^2 = 6.3 \times 10^{-6}$$

$$|\sigma_2| = 0.00031.$$

Figure 16 displays the stochastic volatility density resulting from our approximation to the one in Schorfheide, Song & Yaron (2018).

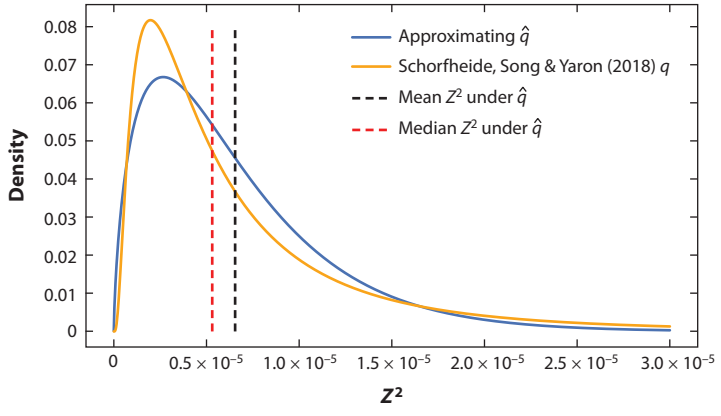

Figure 16

This figure shows two densities for Z^2: the one estimated by Schorfheide, Song & Yaron (2018), q, and the best-fitting one constructed from our minimization problem, $\hat{q}$.

DISCLOSURE STATEMENT

The authors are not aware of any affiliations, memberships, funding, or financial holdings that might be perceived as affecting the objectivity of this review.

ACKNOWLEDGMENTS

We thank Joseph Huang, Chun Hei Hung, Haomin Qin, and Han Xu for excellent research assistance, and Amy Boonstra and Diana Petrova for their oversight of the research support and for editorial assistance. We gratefully acknowledge the Macro-Finance Modeling initiative for their generous financial support. We thank Manav Chaudary, Hui Chen (the Co-Editor), Peter Hansen, Elisabeth Proehl, Simon Scheidegger, Panagiotis Souganidis, Judy Yue, and an anonymous referee for their constructive feedback. In addition, we thank conference participants at the 2nd Macroeconomic Modelling and Model Comparison Network (MMCN), the Platform for Advanced Scientific Computing (PASC18), the University of Zurich, Northwestern University, and the International Joint Conference on Computational and Financial Econometrics (CFE) and Computational and Methodological Statistics (CMStatistics).

LITERATURE CITED

Achdou Y, Han J, Lasry JM, Lions PL, Moll B. 2022. Income and wealth distribution in macroeconomics: a continuous-time approach. *Rev. Econ. Stud.* 89(1):45–86

Al-Aradi A, Correia A, Jardim G, de Freitas Naiff D, Saporito Y. 2022. Extensions of the deep Galerkin method. *Appl. Math. Comput.* 430:127287

Andrei D, Hasler M, Jeanneret A. 2019. Asset pricing with persistence risk. *Rev. Econ. Stud.* 32(7):2809–49

Bansal R, Yaron A. 2004. Risks for the long run: a potential resolution of asset pricing puzzles. *J. Finance* 59(4):1481–509

Barles G, Souganidis PE. 1991. Convergence of approximation schemes for fully nonlinear second order equations. *Asymptot. Anal.* 4(3):271–83

Barnett M, Brock W, Hansen LP, Hu R, Huang J. 2023. *A deep learning analysis of climate change, innovation, and uncertainty*. SSRN Work. Pap. 4607233

Basak S, Cuoco D. 1998. An equilibrium model with restricted stock market participation. *Rev. Financ. Stud.* 11(2):309–41

Bianchi J. 2011. Overborrowing and systemic externalities in the business cycle. *Am. Econ. Rev.* 101(7):3400–26

Borovička J, Hansen LP, Scheinkman JA. 2014. Shock elasticities and impulse responses. *Math. Financ. Econ.* 8:333–54

Brock WA, Magill MJ. 1979. Dynamics under uncertainty. *Econometrica* 47(4):843–68

Brock WA, Mirman L. 1972. Optimal economic growth and uncertainty: the discounted case. *J. Econ. Theory* 4(3):479–513

Brunnermeier MK, Sannikov Y. 2014. A macroeconomic model with a financial sector. *Am. Econ. Rev.* 104(2):379–421

Brunnermeier MK, Sannikov Y. 2015. International credit flows and pecuniary externalities. *Am. Econ. J. Macroecon.* 7(1):297–338

Brunnermeier MK, Sannikov Y. 2016. *The I theory of money*. NBER Work. Pap. 22533

Cerreia-Vioglio S, Hansen LP, Maccheroni F, Marinacci M. 2024. *Making decisions under model misspecification*. Work. Pap., Bocconi Univ., Milan, Italy, Univ. Chicago, Chicago, IL

Chen H, Dou WW, Kogan L. 2024. Measuring "dark matter" in asset pricing models. *J. Finance* 79(2):843–902

Chen Z, Epstein L. 2002. Ambiguity, risk, and asset returns in continuous time. *Econometrica* 70(4):1403–43

Christiano LJ, Motto R, Rostagno M. 2014. Risk shocks. *Am. Econ. Rev.* 104(1):27–65

Cochrane J, Longstaff FA, Santa-Clara P. 2008. Two trees. *Rev. Financ. Stud.* 21(1):347–85

Cox JC, Ingersoll JE Jr., Ross SA. 1985. An intertemporal general equilibrium model of asset prices. *Econometrica* 53(2):363–84

Crouzet N, Eberly JC, Eisfeldt AL, Papanikolaou D. 2022. The economics of intangible capital. *J. Econ. Perspect.* 36(3):29–52
d'Avernas A, Petersen D, Vandeweyer Q. 2022. *A solution method for continuous-time models*. Work. Pap., Stockholm Sch. Econ., Swed.
Di Tella S. 2017. Uncertainty shocks and balance sheet recessions. *J. Political Econ.* 125(6):2038–81
Di Tella S. 2019. Optimal regulation of financial intermediaries. *Am. Econ. Rev.* 109(1):271–313
Dou WW, Lo AW, Muley A, Uhlig H. 2020. Macroeconomic models for monetary policy: a critical review from a finance perspective. *Annu. Rev. Financ. Econ.* 12:95–140
Drechsler I, Savov A, Schnabl P. 2018. A model of monetary policy and risk premia. *J. Finance* 73(1):317–73
Duarte V, Duarte D, Silva D. 2023. *Machine learning for continuous-time finance*. SSRN Work. Pap. 3012602
Duffie D, Epstein LG. 1992. Stochastic differential utility. *Econometrica* 60(2):353–94
Dumas B, Uppal R, Wang T. 2000. Efficient intertemporal allocations with recursive utility. *J. Econ. Theory* 93(2):240–59
Eberly JC, Wang N. 2009. Capital reallocation and growth. *Am. Econ. Rev.* 99(2):560–66
Eberly JC, Wang N. 2011. *Reallocating and pricing illiquid capital: two productive trees*. Work. Pap., Columbia Univ., New York, NY, Northwestern Univ., Evanston, IL
Fournié E, Lasry JM, Lebuchoux J, Lions PL, Touzi N. 1999. Applications of Malliavin calculus to Monte Carlo methods in finance. *Finance Stoch.* 3(4):391–412
Gallant AR, Rossi PE, Tauchen G. 1993. Nonlinear dynamic structures. *Econometrica* 61(4):871–907
Gârleanu N, Panageas S. 2015. Young, old, conservative, and bold: the implications of heterogeneity and finite lives for asset pricing. *J. Political Econ.* 123(3):670–85
Gârleanu N, Pedersen LH. 2011. Margin-based asset pricing and deviations from the law of one price. *Rev. Financ. Stud.* 24(6):1980–2022
Gertler M, Karadi P. 2011. A model of unconventional monetary policy. *J. Monet. Econ.* 58(1):17–34
Gertler M, Kiyotaki N. 2010. Financial intermediation and credit policy in business cycle analysis. In *Handbook of Monetary Economics*, Vol. 3, ed. BM Friedman, M Woodford, pp. 547–99. Amsterdam: Elsevier
Gertler M, Kiyotaki N. 2015. Banking, liquidity, and bank runs in an infinite horizon economy. *Am. Econ. Rev.* 105(7):2011–43
Good IJ. 1952. Rational decisions. *J. R. Stat. Soc. B* 14(1):107–14
Gopalakrishna G. 2022. *A macro-finance model with realistic crisis dynamics*. Work. Pap., Univ. Toronto, Can.
Gromb D, Vayanos D. 2002. Equilibrium and welfare in markets with financially constrained arbitrageurs. *J. Financ. Econ.* 66(2–3):361–407
Haddad V. 2014. *Concentrated ownership and equilibrium asset prices*. Work. Pap., Princeton Univ., Princeton, NJ
Hansen LP. 2007. Beliefs, doubts and learning: valuing macroeconomic risk. *Am. Econ. Rev.* 97(2):1–30
Hansen LP. 2014. Nobel lecture: uncertainty outside and inside economic models. *J. Political Econ.* 122(5):945–87
Hansen LP, Sargent TJ. 2021. Macroeconomic uncertainty prices when beliefs are tenuous. *J. Econometr.* 223(1):222–50
Hansen LP, Sargent TJ. 2022. Structured ambiguity and model misspecification. *J. Econ. Theory* 199:1–32
Hansen LP, Sargent TJ. 2023. Risk, ambiguity, and misspecification: decision theory, robust control, and statistics. *J. Appl. Econometr.* In press. **https://doi.org/10.1002/jae.3010**
Hansen LP, Szőke B, Han LS, Sargent TJ. 2020. Twisted probabilities, uncertainty, and prices. *J. Econometr.* 216(1):151–74
Hayashi F. 1982. Tobin's marginal *q* and average *q*: a neoclassical interpretation. *Econometrica* 50(1):213–24
He Z, Krishnamurthy A. 2011. A model of capital and crises. *Rev. Econ. Stud.* 79(2):735–77
He Z, Krishnamurthy A. 2013. Intermediary asset pricing. *Am. Econ. Rev.* 103(2):732–70
He Z, Krishnamurthy A. 2019. A macroeconomic framework for quantifying systemic risk. *Am. Econ. J. Macroecon.* 11(4):1–37
Hugonnier J. 2012. Rational asset pricing bubbles and portfolio constraints. *J. Econ. Theory* 147(6):2260–302
Jacobson DH. 1973. Optimal stochastic linear systems with exponential performance criteria and their relation to deterministic differential games. *IEEE Trans. Autom. Control* 18(2):124–31
James MR. 1992. Asymptotic analysis of nonlinear stochastic risk-sensitive control and differential games. *Math. Control Signals Syst.* 5(4):401–17

Jermann UJ. 1998. Asset pricing in production economies. *J. Monet. Econ.* 41(2):257–75
Jones LE, Manuelli R. 1990. A convex model of equilibrium growth: theory and policy implications. *J. Political Econ.* 98(5, Part 1):1008–38
Khorrami P. 2020. *The risk of risk-sharing: diversification and boom-bust cycles*. Work. Pap., Imperial College, London
Khorrami P. 2021. *Entry and slow-moving capital: using asset markets to infer the costs of risk concentration*. SSRN Work. Pap. 2777747
Khorrami P, Mendo F. 2023. *Rational sentiments and financial frictions*. Work. Pap., Duke Univ., Durham, NC
Klimenko N, Pfeil S, Rochet JC, De Nicolo G. 2016. *Aggregate bank capital and credit dynamics*. SSRN Work. Pap. 2801995
Koop G, Pesaran MH, Potter SM. 1996. Impulse response analysis in nonlinear multivariate models. *J. Econometr.* 74(1):119–47
Kozak S. 2022. Dynamics of bond and stock returns. *J. Monet. Econ.* 126:188–209
Kreps DM, Porteus EL. 1978. Temporal resolution of uncertainty and dynamic choice. *Econometrica* 46(1):185–200
Krishnamurthy A, Li W. 2021. *Dissecting mechanisms of financial crises: intermediation and sentiment*. NBER Work. Pap. 27088
Lucas RE. 1978. Asset prices in an exchange economy. *Econometrica* 46(6):1429–45
Lucas RE, Prescott EC. 1971. Investment under uncertainty. *Econometrica* 39(5):659–81
Maccheroni F, Marinacci M, Rustichini A. 2006. Ambiguity aversion, robustness, and the variational representation of preferences. *Econometrica* 74(6):1147–498
Martin I. 2013. Lucas orchard. *Econometrica* 81(1):55–111
Maxted P. 2024. A macro-finance model with sentiment. *Rev. Econ. Stud.* 91(1):438–75
Mendo F. 2018. *Risk to control risk*. Work. Pap., Princeton Univ., Princeton, NJ
Mendoza EG. 2010. Sudden stops, financial crises, and leverage. *Am. Econ. Rev.* 100(5):1941–66
Merton RC. 1973. An intertemporal capital asset pricing model. *Econometrica* 41(5):867–87
Moreira A, Savov A. 2017. The macroeconomics of shadow banking. *J. Finance* 72(6):2381–432
Panageas S. 2020. The implications of heterogeneity and inequality for asset pricing. *Found. Trends Finance* 12(3):199–275
Petersen IR, James MR, Dupuis P. 2000. Minimax optimal control of stochastic uncertain systems with relative entropy constraints. *IEEE Trans. Autom. Control* 45:398–412
Phelan G. 2016. Financial intermediation, leverage, and macroeconomic instability. *Am. Econ. J. Macroecon.* 8(4):199–224
Schorfheide F, Song D, Yaron A. 2018. Identifying long-run risks: a Bayesian mixed-frequency approach. *Econometrica* 86(2):617–54
Silva DH. 2016. *The risk channel of unconventional monetary policy*. Work. Pap., MIT, Cambridge, MA
Whittle P. 1981. Risk-sensitive linear/quadratic/Gaussian control. *Adv. Appl. Probab.* 13(4):764–77